DOKUZ EYLÜL UNIVERSITY
GRADUATE SCHOOL OF NATURAL AND APPLIED SCIENCES

OPTICAL SIGNAL PROCESSING FOR ALL-OPTICAL COMPUTER NETWORKS

by
Bora MOCAN

December, 2009
İZMİR

OPTICAL SIGNAL PROCESSING FOR ALL-OPTICAL COMPUTER NETWORKS

A Thesis Submitted to the
Graduate School of Natural and Applied Sciences of Dokuz Eylül University
In Partial Fulfillment of the Requirements for the Degree of Doctor of Philosophy
in
Electrical and Electronics Engineering

by
Bora MOCAN

December, 2009
İZMİR

Ph.D. THESIS EXAMINATION RESULT FORM

We have read the thesis entitled **"OPTICAL SIGNAL PROCESSING FOR ALL-OPTICAL COMPUTER NETWORKS"** completed by **BORA MOCAN** under supervision of **YRD DOÇ. DR. ZAFER DICLE** and we certify that in our opinion it is fully adequate, in scope and in quality, as a thesis for the degree of Doctor of Philosophy.

Yrd. Doç. Dr. Zafer Dicle

Supervisor

Prof. Dr. Ufuk Çağlayan	Prof. Dr. Mustafa Gündüzalp
Thesis Committee Member	Thesis Committee Member
Examining Committee Member	Examining Committee Member

Prof.Dr. Cahit HELVACI
Director
Graduate School of Natural and Applied Sciences

ACKNOWLEDGEMENTS

Foremost, I would like to thank my co-supervisor, Doç. Dr. M. Salih Dinleyici, who shared with me a lot of his expertise and research insight. He quickly became for me the role model of a successful researcher in the field. And I am deeply grateful to Yrd. Doç. Dr. Zafer Dicle and Prof. Dr. Ufuk Çağlayan for their support.

I wish to thank everybody with whom I have shared experiences in life. From the people who first persuaded and got me interested into the study of electronics.

I am tempted to individually thank all of my friends which, from my childhood until graduate school, have joined me in the discovery of what is life about and how to make the best of~it. However, because the list might be too long and by fear of leaving someone out, I will simply say thank you very much to you all.

I cannot finish without saying how grateful I am with my family: my wife Nejla, my parents, my friends all have given me a loving environment where to develop. They have always supported and encouraged me to do my best in all matters of life. To them I dedicate this thesis.

Bora Mocan

OPTICAL SIGNAL PROCESSING FOR
ALL-OPTICAL COMPUTER NETWORKS

ABSTRACT

Optical networks are evolving from static optical circuits and subsequently optical circuit switching towards optical packet switching in order to take advantage of the high transport capacity made available by WDM and OTDM systems in a more flexible way.

Optically labeling of packets and routing the packets's payload optically under control of its label allows the network nodes to route and forward IP data without having to process the payload, thus keeping it in the optical domain; this is a promising solution to avoid electronic bottlenecks in routers. All-optical label switching can therefore be used to route and forward packets independent of their length and payload bitrate.

This thesis studies optical signal processing techniques, its potential applications and a novel all-optical routing architecture.

Keywords: Optical signal processing, optical networks, optical routing, optical switching, optical header recognition.

TÜM-OPTİK BİLGİSAYAR AĞLARI İÇİN OPTİK SİNYAL İŞLEME

ÖZ

Optik ağlar, WDM ve OTDM sistemlerinin avantajlarını kullanmak ve yüksek kapasitelere ulaşmak için statik optik bağlantı yapılarından tamamen optik anahtarlamalı sistemlere doğru evrimleşmektedir. Veri paketlerinin optik olarak etiketlenmesi ve bu etiketler yardımıyla tamamen optik düzlemde işlenip yönlendirilmesi, ağ yapılarını sınırlandıran en büyük etken olan elektronik-optik dönüşümünü ortadan kaldıracaktır. Tüm-optik etiket anahtarlama veri paketlerini içeriğinden ve protokolden bağımsız olarak yönlendirme ve iletme özelliğine sahip olabilir.

Bu tezde optik sinyal işleme elemanları, potansiyel uygulamaları ve yeni bir tüm-optik yönlendirme mimarisi işlenmiştir.

Anahtar Kelimeler: Optik sinyal işleme, optik ağ yapıları, optik yönlendirme, optik anahtarlama, optik başlık tanıma ve ayrıştırma.

CONTENTS

Page

Page

Page

CHAPTER ONE
INTRODUCTION

In this thesis, a novel all-optical routing architecture based on available optical techniques and devices, is proposed. The design relies upon self-routing of the optical data packets using the packet's address information and the routing table of the network topology. Network protocols with smaller and simpler routing tables have high potential to accommodate this design. Especially latest, popular network protocols such as Multi Protocol Label Switching (MPLS) and Internet Protocol version six (IPv6) data packets might be very efficiently routed by this technique.

IPv6 has much larger address space (128 bits) than IPv4 (32 bits), which enables the use of multiple levels of hierarchy inside the address space. Each level helps to aggregate its IP space and enhance the allocation function. Service providers and organizations may have a tiered hierarchy (Desmeu, 2003). It means there are fewer routes to analyze, fewer fields to process, and fewer decisions to make in forwarding a data packet (Davies, 2003).

MPLS is another forwarding technique in autonomous networks that may accommodate this approach for optimizing the routing process (Tomsu & Schmutzer, 2002). Global network reachability is handled at the edge and packet forwarding rules are propagated to the core network. Label Edge Routers (LER) work as interface between the MPLS network and IP Internet and assign simple labels for the incoming packet streams. A MPLS network consists of Label Switch Routers (LSR) in the core of the network. Within the MPLS network, traffic is forwarded via LSRs just using the labels. MPLS and IPv6 are designed to improve the routing and switching bottlenecks of the current Internet Protocol (IPv4). Therefore, the novel routing architecture proposed here might be adapted for both IPv6 and MPLS networks (Tomsu & Schmutzer, 2002).

Optical buffers, optical switches, header recognition, and route decision units are key building blocks of a general optical routing node. Truly photonic routers require

photonic implementations of all these functions. The lack of all-optical processors and random access memories force designers to implement specific signal processing algorithms in separate optical modules. However, the interactions among these models should be carefully considered to overcome the synchronization and stability problems that may arise on ultra-fast data rates. The use of fixed length packets can, however, significantly simplify the implementation of packet content resolution and buffering as well as packet synchronization (Dinleyici & Mocan, 2002), (Mocan & Dinleyici, 2003).

CHAPTER TWO
OPTICAL NETWORKS

2.1 Overview

Optical networks are high-capacity telecommunications networks based on optical technologies and components that provide switching, routing, and amplifying at optical domain. As networks require more and more bandwidth for internet and multimedia applications and network providers are moving to a network evolution: the optical network. Optical networks, provide higher capacity and reduced costs for applications such as the Internet, video and multimedia services, and advanced digital services.

2.2 History of Optical Networks

In the early 1980s, a revolution in telecommunications networks began by the use of a fiber-optic cable. Since then, the huge cost savings and increased network quality has led to many advances in the technologies. Now, optical networks are the requirement, the benefits are unquestionable. Throughout this history, the digital network has evolved in three fundamental and main stages: asynchronous, synchronous, and optical (Tanenbaum, 2003).

2.2.1 Asynchronous Networks

The pioneer digital telecommunication networks were asynchronous networks. In asynchronous networks, each network device has its own internal clock source. Because each clock had a certain amount of time variation, the arrival and the transmitting of the data signals could have a variation in timing. This often results in bit errors. More importantly, as optical-fiber deployment evolved, no standards existed, how network elements should process the optical data. Many different methods appeared, making it difficult for providers to interconnect equipment from different device vendors.

2.2.2 Synchronous Networks

The need for optical standards led to the creation of the SONET (Synchronous Optical NETwork). SONET standardized line rates, coding schemes, bit-rate hierarchies, and operations and maintenance functionality. SONET also defined the types of network elements required, network architectures that vendors could implement, and the functionality that each node must perform. Network providers could now use different vendor's optical equipment with the confidence of at least basic interoperability (Tanenbaum, 2003).

2.2.3 Optical Networks

SONET is based on open-ended growth plan for higher bit rates, theoretically no upper limit exists for bit rates. However, as higher bit rates are used, physical limitations in the laser sources, electronic equipments and optical fiber begin to endlessly increasing the bit rate on each signal an impractical solution. Additionally, connection to the networks through different protocols and the bottleneck on the routing increased requirements. Customers are demanding more services and more bandwidth. Optical networks provide the required bandwidth and flexibility to enable end-to-end wavelength services.

Optical networks began with wavelength division multiplexing (WDM), which provides additional capacity on existing fibers. Like SONET, defined network elements and architectures provide the basis of the optical network. However, unlike SONET, the optical network will be based on wavelengths, rather than using a defined bit rate and data packet structure as. The components of the optical network will be defined according to how the wavelengths are transmitted, received, or implemented in the network.

Viewing the network from a layered approach, networks are divided into several different physical or virtual layers. The first layer, the services layer, is where the services and data traffic enter the telecommunications network. The next layer,

SONET, provides restoration, performance monitoring, and provisioning that is transparent to the first layer. Emerging with the optical network is a third layer, the optical layer, operating entirely in the optical domain. The optical network also has the additional requirement of carrying varied types of high bit-rate nonSONET optical signals that bypass the SONET layer altogether. Just as the SONET layer is transparent to the services layer, the optical layer will ideally be transparent to the SONET layer, providing restoration, performance monitoring, and provisioning of OTDM(Optical Time Division Multiplexing) and instead of electrical SONET signals (Walrand & Varaiya, 2000).

2.3 Advantages of Optical-Networks

Many factors are driving the need for optical networks. A few of the most important reasons for migrating to the optical layer are described.

2.3.1 Fiber Capacity

The first implementation of what has emerged as the optical network began on routes that were fiber limited. Providers needed more capacity between two sites, but higher bit rates or fibers were not available. The only options in these situations were to install more fiber, which is an expensive and labor-intensive chore, or place more time division multiplexed (TDM) signals on the same fiber. WDM provided many virtual fibers on a single physical fiber. By transmitting each signal at a different frequency, network providers could send many signals on one fiber just as though they were each traveling on their own fiber.

2.3.2 Restoration Capability

As network planners use more network elements to increase fiber capacity, a fiber cut can have massive implications. In current electrical architectures, each network element performs its own restoration. For a WDM system with many channels on a single fiber, a fiber cut would initiate multiple failures, causing many

independent systems to fail. By performing restoration in the optical layer rather than the electrical layer, optical networks can perform protection switching faster and more economically. Additionally, the optical layer can provide restoration in networks that currently do not have a protection scheme. By implementing optical networks, providers can add restoration capabilities to embedded asynchronous systems without first upgrading to an electrical-protection scheme.

2.3.3 Reduced Cost

In systems using only WDM, each location that demultiplexes signals will need an electrical network element for each channel, even if no traffic is dropping at that site. By implementing an optical network, only those wavelengths that add or drop traffic at a site need corresponding electrical nodes. Other channels can simply pass through optically, which provides tremendous cost savings in equipment and network management. In addition, performing space and wavelength routing of traffic avoids the high cost of electronic cross-connects, and network management is simplified.

2.3.4 Wavelength Services

One of the great revenue-producing aspects of optical networks is the ability to resell bandwidth rather than fiber. By maximizing capacity available on a fiber, service providers can improve revenue by selling wavelengths, regardless of the data rate required. To customers, this service provides the same bandwidth as a dedicated fiber.

2.4. Enabling Technologies

The cornerstone of an optical network is the advanced optical technologies that perform the necessary all-optical functions. Optical technologies continue to advance by various techniques and implementations to improve the performance and capabilities of the optical network.

As fiber optics came into use, network providers soon found that some improvements in technology could greatly increase capacity and reduce cost in existing networks. These early technologies eventually led to the optical network as it is today.

2.4.1 WDM and DWDM

The first incarnation of WDM was broadband WDM. In 1994, by using fused biconic tapered couplers, two signals could be combined on the same fiber. Because of limitations in the technology, the signal frequencies had to be widely separated, and systems typically used 1,310-nm and 1,550-nm signals, providing 5 Gbps on one fiber. Although the performance did not compare to today's technologies, the couplers provided twice the bandwidth out of the same fiber, which was a large cost savings compared to installing new fiber.

As optical filters and laser technology improved, the ability to combine more than two signal wavelengths on a fiber became a reality. Dense wavelength division multiplexing (DWDM) combines multiple signals on the same fiber, ranging up to 400 channels. By implementing DWDM systems and optical amplifiers, networks can provide a variety of bit rates (i.e., OC–48 or OC–192), and a multitude of channels over a single fiber. The wavelengths used are all in the range that optical amplifiers perform optimally, typically from about 1,530 nm to 1,565 nm.

Two basic types of DWDM are implemented today: unidirectional and bidirectional DWDM. In a unidirectional system, all the wavelengths travel in the same direction on the fiber, while in a bidirectional system the signals are split into separate bands, with both bands traveling in different directions (Stallings, 2007)

2.4.2 Optical Amplifiers

The second basic technology, and perhaps the most fundamental to today's optical networks, was the erbium-doped optical amplifier. By doping a small strand

of fiber with a rare earth metal, such as erbium, optical signals could be amplified without converting the signal back to an electrical state. The amplifier provided enormous cost savings over electrical regenerators, especially in long-haul networks.

Systems deployed today use devices that perform similar functions to earlier devices but are much more efficient and precise. In particular, flat-gain optical amplifiers have been the true enabler for optical networks by allowing the combination of many wavelengths across a single fiber.

The performance of optical amplifiers has improved significantly—with current amplifiers providing significantly lower noise and flatter gain—which is essential to DWDM systems. The total power of amplifiers also has steadily increased, which is many orders of magnitude more powerful than the first amplifiers (Connelly, 2002).

2.4.3 Narrowband Lasers

Without a narrow, stable, and coherent light source, none of the optical components would be of any value in the optical network. Advanced lasers with narrow bandwidths provide the narrow wavelength source that is the individual channel in optical networks. Typically, long-haul applications use externally modulated lasers, while shorter applications can use integrated laser technologies.

These laser sources emit a highly coherent signal that has an extremely narrow bandwidth. Depending on the system used, the laser may be part of the DWDM system or embedded in the SONET network element. When the precision laser is embedded in the SONET network element, the system is called an embedded system. When the precision laser is part of the WDM equipment in a module called a transponder, it is considered an open system because any low-cost laser transmitter on the SONET network element can be used as input (Menzel, 2001).

2.4.4 Fiber Bragg Gratings

Commercially available fiber Bragg gratings have been important components for enabling WDM and optical networks. A fiber Bragg grating is a small section of fiber that has been modified to create periodic changes in the index of refraction. Depending on the space between the changes, a certain frequency of light—the Bragg resonance wavelength—is reflected back, while all other wavelengths pass through. The wavelength-specific properties of the grating make fiber Bragg gratings useful in implementing optical add/drop multiplexers. Bragg gratings also are being developed to aid in dispersion compensation and signal filtering as well.

2.4.5 Thin Film Substrates

Another essential technology for optical networks is the thin film substrate. By coating a thin glass or polymer substrate with a thin interference film of dielectric material, the substrate can be made to pass through only a specific wavelength and reflect all others. By integrating several of these components, many optical network devices are created, including multiplexers, demultiplexers, and add/drop devices (Menzel, 2001).

2.4.6 Semiconductor Optical Amplifier (SOA) Applications

Key functions have been identified as requirements for the emerging optical network. As component technologies advance, each of the functions required, such as tunable filters, space switches, and wavelength converters, will become more cost effective and practical.

One of the most promising technologies for optical networks is the semiconductor optical amplifier (SOA). By integrating the amplifier functionality into the semiconductor material, the same basic component can perform many different applications. SOAs can provide integrated functionality of internal switching and routing functions that are required for a feature-rich network. Space

switches, wavelength converters, and wavelength selectors all can be made from SOAs, which will lead to large cost reductions and improved performance in future optical-network equipment.

Promising new gain-switching technology makes possible optical-space switches, selectable filters, and wavelength converters. Today's transmission systems employ NRZ at OC–48 (2.5 Gbps) and OC–192 (10 Gbps) data rates. However, new transmission technologies are being studied to open the way to OC–768 (40 Gbps). These new systems might be based on either electronic time division multiplexing (ETDM) or optical time division multiplexing (OTDM) 4X10–Gbps technologies. Advances are being made with integrated laser modulators that provide lower-cost narrowband transmitters (Odom, 2006).

2.4.7 Soliton

Soliton transmission, first deployed in submarine links, might find application in terrestrial networks to improve transmission performance or in some types of all-optical signal processing such as 3R regeneration. Research dealing with polarization-mode dispersion mitigation, phase-shaped binary transmission (PSBT), and fiber-grating technologies promise significant advances in the near future with regard to increasing system performance and network capacity (Saleh & Teich, 1991).

All of these technologies aim to reduce the network cost and provide valuable new services to customers who are constantly demanding more bandwidth-intensive and flexible features from their network providers.

CHAPTER THREE
SEMICONDUCTOR OPTICAL AMPLIFIERS (SOA)

3.1 Overview

The rapid growth of the optical communication networks has been made possible by the development of new optoelectronic technologies that can use the enormous bandwidth of optical fiber. Today, systems are operational at bit rates 100 Gb/s. Almost any kind of communication services are carried by optical networks; and to achieve full transparency that allows flexible routing of channels all optical communication networks should be used.

Many of the advances in optical networks have been made possible by the optical amplifiers. Optical amplifiers can be divided into two classes: optical fiber amplifiers (OFAs) and semiconductor optical amplifiers (SOAs). OFA has tended to dominate conventional system applications such as in-line amplification used to compensate for fiber losses. However, due to advances in optical semiconductor fabrication techniques and device design, the SOA is showing great potential for use in evolving optical communication networks. It can be utilized as a general gain element but also has many functional applications including optical switching, wavelength conversion, multiplexing and optical logic gate design. These functions, where there is no conversion of optical signals into the electrical domain, are required in transparent optical networks. This chapter summarizes SOA technology and the applications of SOAs in optical communication and its simulations will be given in detail.

3.2 How SOA operates?

A schematic diagram of an SOA is shown in Figure 3.1. The device is driven by an electrical current. The active region in the device produces gain, via stimulated emission, to an input signal (Figure 3.2). The output signal is accompanied by noise.

This additive noise, amplified spontaneous emission (ASE), is produced by the amplification process. A comparison between OFAs and SOAs is given in Table 3.1.

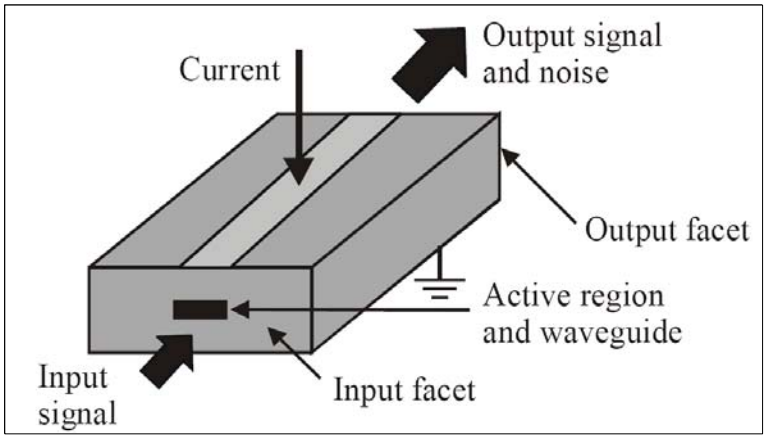

Figure 3.1 Schematic diagram of SOA

SOAs are polarization sensitive. This is due to a number of factors including the waveguide structure and the gain material. Polarization sensitivity can be improved by the use of square-cross section waveguides and strained quantum-well material (Connely, 2002).

The gain of an SOA is influenced by the input signal power and internal noise generated by the amplification process. As the input signal power increases the gain decreases. The gain saturation can cause significant signal distortion. It can also limit the gain achievable when SOAs are used as multichannel amplifiers in wavelength division (WDM) multiplexed systems.

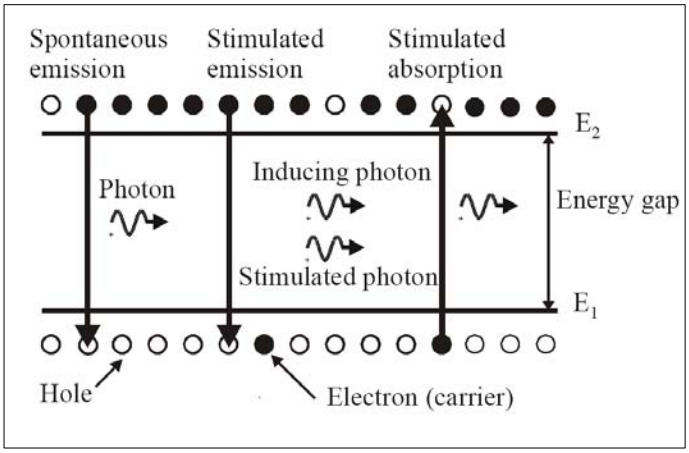

Figure 3.2 Spontaneous and stimulated processes in a two level system.

Table 3.1 Comparison between OFAs and SOAs (www.iec.org.tr, 2006).

Feature	**OFA**	**OSA**
Maximum internal gain (dB)	30 - 50	30
Insertion loss (dB)	0.1 - 2	6 - 10
Polarization sensitive?	No	Weak (< 2 dB)
Pump source	Optical	Electrical
3 dB gain bandwidth (nm)	30	30 - 50
Nonlinear effects	Negligible	Yes
Saturation output power (dBm)	10 - 15	5 - 20
Noise figure (dB)	3 - 5	7 - 12 dBm
Integrated circuit compatible	No	Yes
Functional device possibility	No	Yes
Maximum internal gain (dB)	30 - 50	30
Insertion loss (dB)	0.1 - 2	6 - 10

SOAs are normally used to amplify modulated light signals. If the signal power is high then gain saturation will occur. This would not be a serious problem if the amplifier gain dynamics were a slow process (IEC, 2006).

However in SOAs the gain dynamics are determined by the carrier recombination lifetime (few hundred picoseconds). This means that the amplifier gain will react relatively quickly to changes in the input signal power. This dynamic gain can cause signal distortion, which becomes more severe as the modulated signal bandwidth increases. These effects are even more important in multichannel systems where the dynamic gain leads to interchannel crosstalk. This is in contrast to optical fiber amplifiers, which have recombination lifetimes of the order of milliseconds leading to negligible signal distortion (Giller, 2006).

SOAs also exhibit nonlinear behavior. These nonlinearities can cause problems such as frequency chirping and generation of intermodulation products. However, nonlinearities can also be of use in using SOAs as functional devices such as wavelength converters (Liu, 2007).

3.3 Amplifier Applications of SOA

The principal applications of SOAs in optical communication systems can be classified into three areas:

(a) Post-amplifier or booster amplifier to increase transmitter laser power,

(b) In-line amplifier to compensate for fiber and other transmission losses in medium and long-haul links and

(c) Pre-amplifier to improve receiver sensitivity (Figure 3.3).

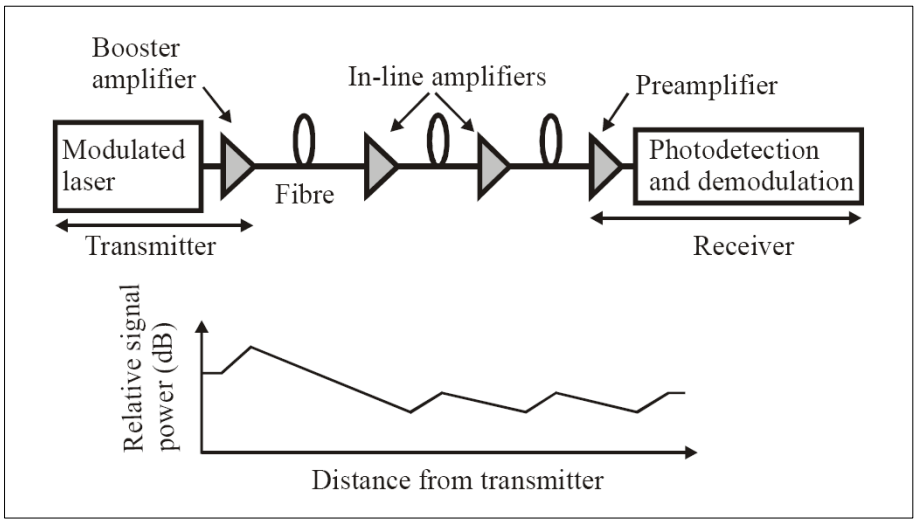

Figure 3.3 Application of SOAs as booster amplifier, in-line amplifiers and preamplifier in an optical transmission link.

The incorporation of optical amplifiers into optical communication links can improve system performance and reduce costs. The main requirements of optical amplifiers for such applications are listed in Table 3.2 (IEC, 2006).

Table 3.2 Optical amplifier requirements

	Post-Amplifier	**In-Line Amplifier**	**Pre-Amplifier**
High Gain	Yes	Yes	Yes
High Saturation Output Power	Yes	Yes	Not Critical
Low Noise Figure	Not Critical	Yes	Yes
Low Polarization Sensitivity	Not Critical	Yes	Yes
Low Insertion Loss	Not Critical	Yes	Yes
Optical Filter	Not Critical	Not Critical	Yes
Optical Isolators	Yes	Not Critical	Not Critical

3.3.1 Booster Amplifier

The function of a booster amplifier is to increase a high power input signal before transmission. The principle applications of booster amplifiers are listed as:

- Increase medium-haul optical transmission link distance
- Increase long-haul optical transmission link power budget
- Compensate for splitting and tap losses in optical distribution networks
- Simultaneous amplification of WDM signals

Boosting laser power in an optical transmitter enables the construction of medium-haul links with increased transmission distance. Such links simply consist of an optical fiber between the transmitter and receiver. As this involves there is no need for active components in the transmission link. The reliability and performance of the links are improved. In long-haul links the use of a booster amplifier can increase the link power budget and reduce the number of in-line amplifiers or regenerators required. Booster amplifiers are also useful in distribution networks (Figure 3.4), where there is large splitting losses or a large number of taps. Booster amplifiers are also needed to simultaneously amplify a number of input signals at different wavelengths (e.g. WDM transmission) (Spiekman, 2000).

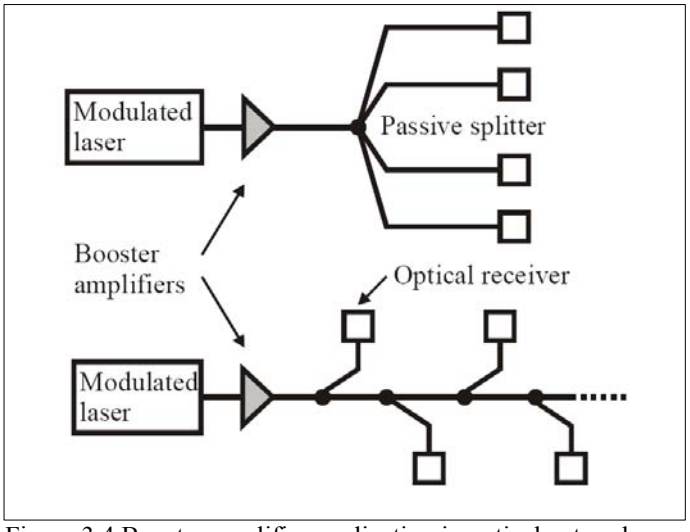

Figure 3.4 Booster amplifier application in optical networks.

3.3.2 Pre-Amplifier

The function of an optical preamplifier is to increase the power level of an optical data signal before to detection and demodulation. The increase in power level can increase receiver sensitivity. This allows longer unrepeated links. A schematic diagram of a pre-amplified optical receiver is shown in Figure 3.5. The receiver consists of an optical preamplifier, a narrowband optical filter and photodiode followed by post-detection circuitry and a decision circuit (Spiekman, 2000).

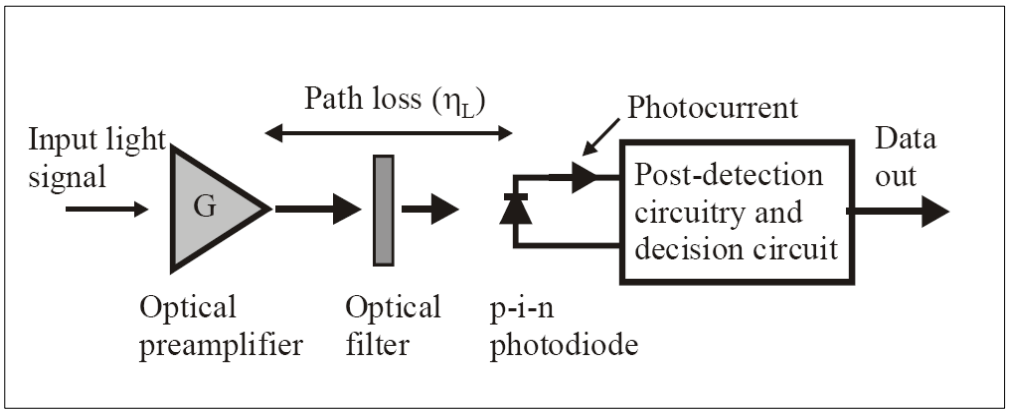

Figure 3.5 Preamplified optical filter.

3.3.3 In-Line Amplifier

In loss limited optical communication systems, in-line optical amplifiers can be used to compensate for fiber loss and overcoming the need for optical regeneration. The main advantages of in-line SOAs are: Transparency to data rate and modulation format (unsaturated operation and at high bit rates), bi-directionality, WDM capability, simple mode of operation, low power consumption and compactness. The latter two advantages are important for remotely located optical components (Spiekman, 2000).

3.4 SOA Nonlinearities and Nonlinear Usage

SOAs can also be used to perform functions that are useful in optically transparent networks. These all-optical functions can help to overcome the

'electronic bottleneck'. This is a major limiting factor in the deployment of high-speed optical communication networks. Many of these functional applications are based on SOA nonlinearities. The development of photonic integrated circuits has made feasible the deployment of complex SOA functional subsystems. Nonlinearities in SOAs are principally caused by carrier density changes induced by the amplifier input signals. The four main types of nonlinearity are: Cross gain modulation (XGM), cross phase modulation (XPM), self-phase modulation (SPM) and four-wave mixing (FWM) (Connely, 2002).

3.4.1 Cross Gain Modulation(XGM)

The material gain spectrum of an SOA is homogenously broadened. This means that carrier density changes in the amplifier will affect all of the input signals, so it is possible for a strong signal at one wavelength to affect the gain of a weak signal at another wavelength. This non-linear mechanism is called XGM. The most basic XGM scenario is shown in Fig. 8, where a weak CW probe light and a strong pump light, with a small-signal harmonic modulation at angular frequency ω, are injected into an SOA. XGM in the amplifier will impose the pump modulation on the probe. This means that the amplifier is acting as a wavelength converter.

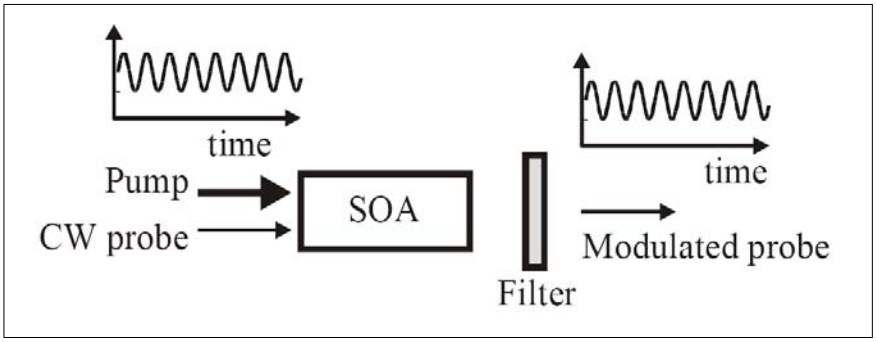

Figure 3.6 Simple wavelength converter using SOA XGM

The most useful figure of merit of the converter is the conversion efficiency, defined as the ratio between the modulation indexes of the output probe to the modulation index of the input pump. Typical efficiency bandwidths are of the order of 10 GHz.

3.4.2 Cross Phase Modulation(XPM)

The refractive index of an SOA active region is not constant but is dependent on the carrier density and so the material gain. This implies that the phase and gain of an optical wave propagating through the amplifier are coupled via gain saturation. This strength of this coupling is related to the linewidth enhancement factor α. If more than one signal is injected into an SOA, there will be cross-phase modulation (XPM) between the signals. XPM can be used to create wavelength converters and other functional devices. However, because XPM only causes phase changes, the SOA must be placed in an interferometric configuration to convert phase changes in the signals to intensity changes using constructive or destructive interference.

3.4.3 Four Wave Mixing(FWM)

Four-wave mixing (FWM) is a coherent nonlinear process that can occur in an SOA between two optical fields, a strong pump at angular frequency ω_0 and a weaker signal (or probe) at $\omega_0 - \Omega$, having the same polarization. The injected fields cause the amplifier gain to be modulated at the beat frequency Ω. This gain modulation in turn gives rise to a new field at $\omega_0 + \Omega$, as shown in Figure 3.7. FWM generated in SOAs can be used in many applications including wavelength converters, dispersion compensators and optical demultiplexers.

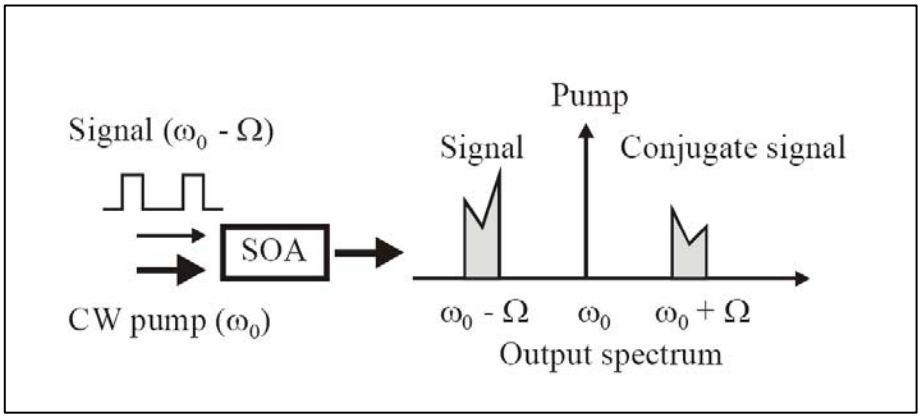

Figure 3.7 SOA FWM(Four Wave Mixing)

3.5 Functional Applications of SOA

3.5.1 Wavelength Conversion

All-optical wavelength converters will play an important role in broadband optical networks. Their most important function will be to avoid wavelength blocking in optical cross-connects in WDM networks. Wavelength converters increase the flexibility and capacity of a network using a fixed set of wavelengths. Wavelength conversion can also be used for network management. In packet switching networks, tunable wavelength converters can be used to resolve packet contention and reduce optical buffering requirements.

XGM in an SOA can be used for wavelength conversion. SOA XPM can also be used for wavelength conversion if SOA's are placed in a Mach-Zehnder configuration as shown in Figure 3.8. These wavelength converters have a superior power efficiency compared to those devices based on XGM (Liu, 2007).

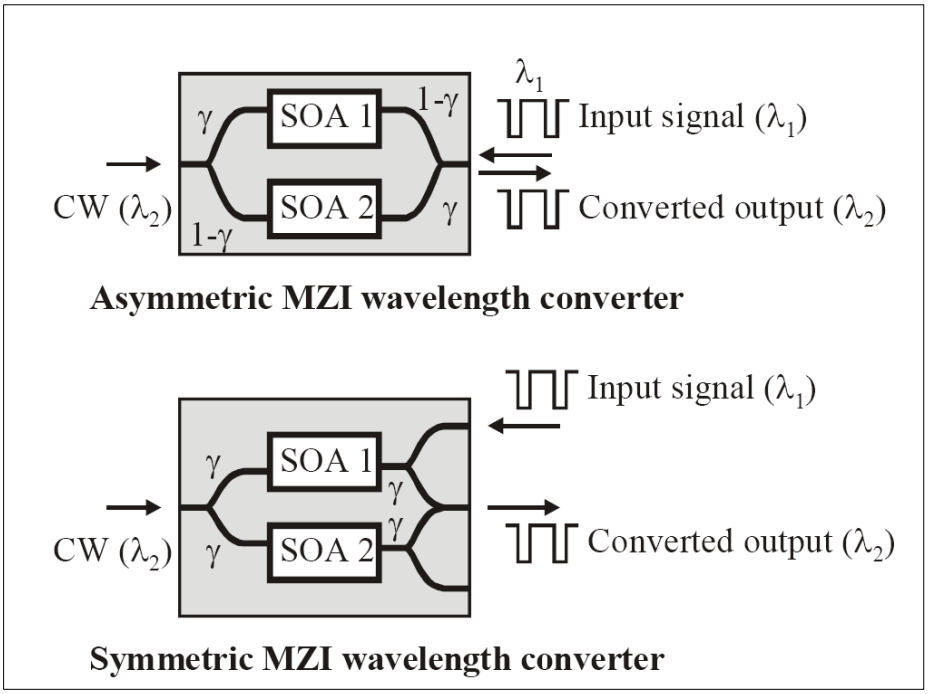

Figure 3.8 Mach-Zehnder interferometer (MZI) SOA wavelength converter.

In the asymmetric MZI wavelength converter the CW input at λ_2 is split asymmetrically to each arm of the MZI by a coupler. The intensity modulated signal at λ_1 saturates each SOA asymmetrically inducing different phase shifts in the input CW signal. The output coupler recombines the split CW signals where they can interfere constructively or destructively. The actual state of interference depends on the relative phase difference between the interferometer arms, which relies both on the SOA bias currents and on the input optical powers (Liu, 2007).

3.5.2 Optical Logic Gates

Future high-speed WDM and TDM optical communication networks require high-speed optical switches (or gates) that can either be optically or electrically controlled. Such optical switches can be constructed using SOAs. The simplest method to control an SOA gate is by turning the device current on or off. The great advantage of SOA gates is that they can be integrated to form gate arrays. In the 2 x 2 switch module shown in Figure 3.9, an incoming data packet can be routed to any output port by switching on the appropriate SOA (Kim, 2006) (Kristian, 2000).

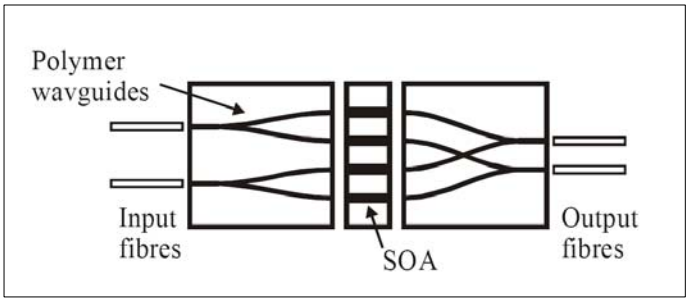

Figure 3.9 Hybrid 2 x 2 SOA switch module.

The switching time of a current switched SOA is of the order of 100 ps. Much faster switching times can be achieved using SOAs placed in non-linear loop mirrors (Figure 3.10). Switching is achieved by placing an SOA offset from the centre of an optical fibre loop mirror and injecting data into the loop via a 50:50 coupler. The two counter-propagating data pulse streams arrive asynchronously at the SOA. A switching pulse is timed to arrive after one data pulse but just before its replica. The switching pulse power is adjusted to impart a phase change of π radians onto the

replica, so the data pulse is switched out when the two counter-propagating components interfere on their return to the coupler. This device is also known as a TOAD (terahertz optical asymmetric demultiplexer) because it can also be used to demultiplex high-speed TDM pulse streams.

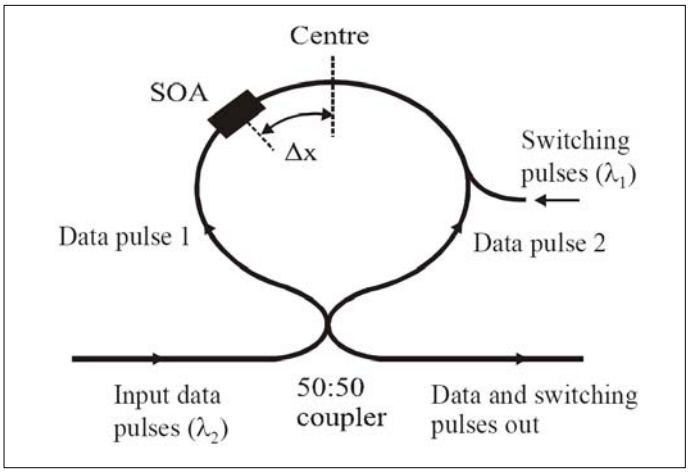

Figure 3.9 Optical switch using a TOAD.

Optical logic can be useful for all-optical signal processing applications in high-speed optical networks. Three SOA configurations that can be used to realise optical logic gates are shown in Figure 3.10.

3.5.3 Multiplexers

Optical time division demultiplexers (OTDMs) and add/drop multiplexers (ADMs) are key components required by optical time division multiplexed (OTDM) network nodes. In an ADM one channel is dropped from an incoming TDM data stream leaving the other channels undisturbed. A new channel can be added by inserting data pulses into the vacant time slot. MZI switches incorporating SOAs can also be used as ADMs. Many configurations are possible, one of which is shown in Figure 3.11. In this configuration the input data signal at 40 Gb/s is split into two drive signals. One of the drive signals is delayed by a half a bit period. The interferometer is configured such that when an undelayed signal pulse is present in the upper arm of the interferometer an input 10 GHz pulse is directed to the drop

port. At the same time the 3 x 10 GHz pulse stream is directed to the through port. (Son, 2006)

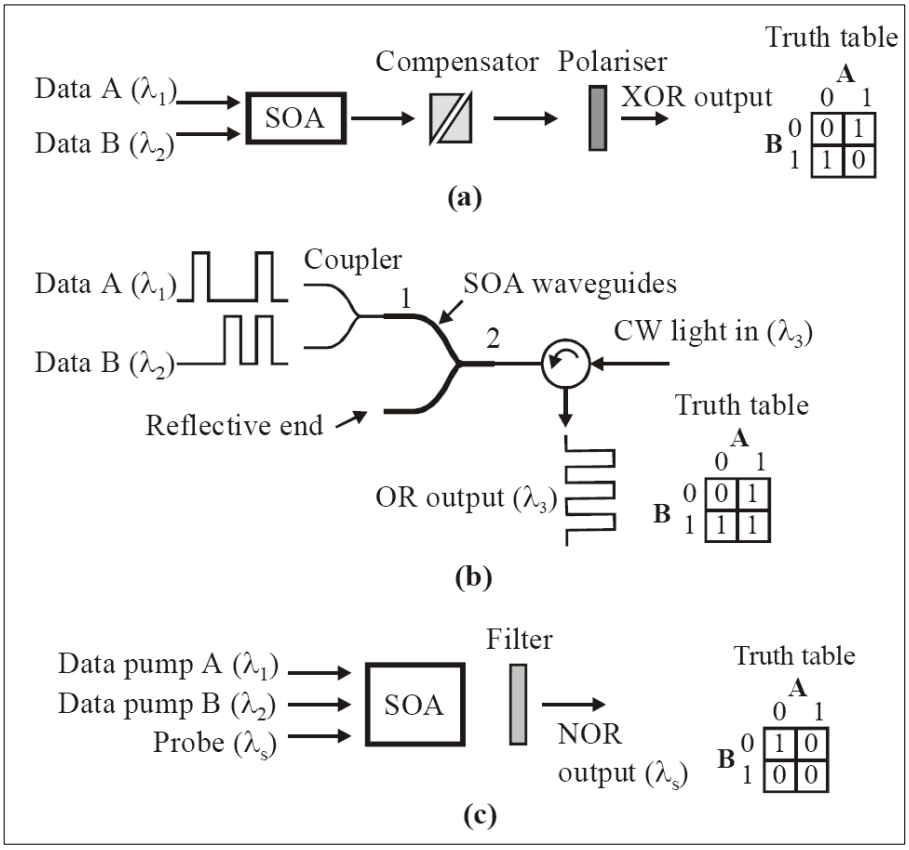

Figure 3.10 SOA logic Gates (a)XOR gate, (b) OR gate, (c) NOR gate.

When the delayed signal pulse is present in the lower arm of the interferometer the data is directed away from the drop port. The amplitudes of the drop and through pulses are modified by the SOA gain saturation induced by the input data pulses so pulse amplification and reshaping also occurs, i.e. the device functions as a 2R regenerator. If it is combined with optical clock recovery for retiming it will function as a 3R regenerator. Data can be added to the vacant time slot in the output data simply by sending the add channel data pulses to the add port (Yang, 2006).

The ability to add and drop wavelength channels in WDM networks is useful for wavelength routing. The function of a wavelength ADM is to separate a particular wavelength channel without interference from adjacent channels. This can be achieved by a wavelength demultiplexer or by using an integrated SOA with a

tuneable filter as shown in Figure 3.12. The filter can be tuned by changing its current. The selected wavelength channel is reflected by the filter, amplified a second time by the MQW section and extracted to a drop port using a circulator. The remaining channels pass through the filter section to which it is a simple matter to add a new wavelength channel (Connelly, 2002).

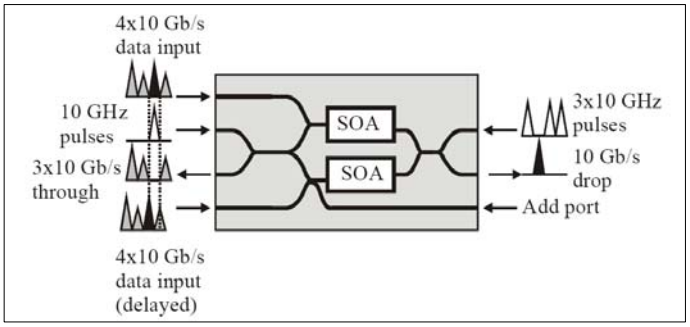

Figure 3.11 Mach Zehnder Add-Drop Multiplexer.

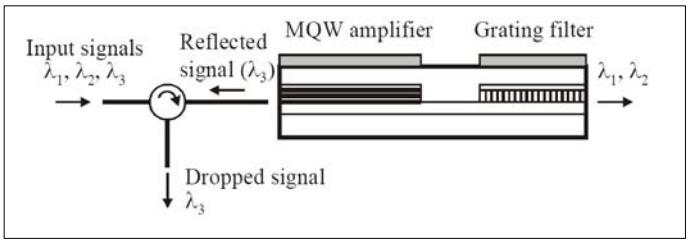

Figure 3.12 Tunable SOA-filter wavelength ADM.

3.5.4 All-Optical Clock Recovery

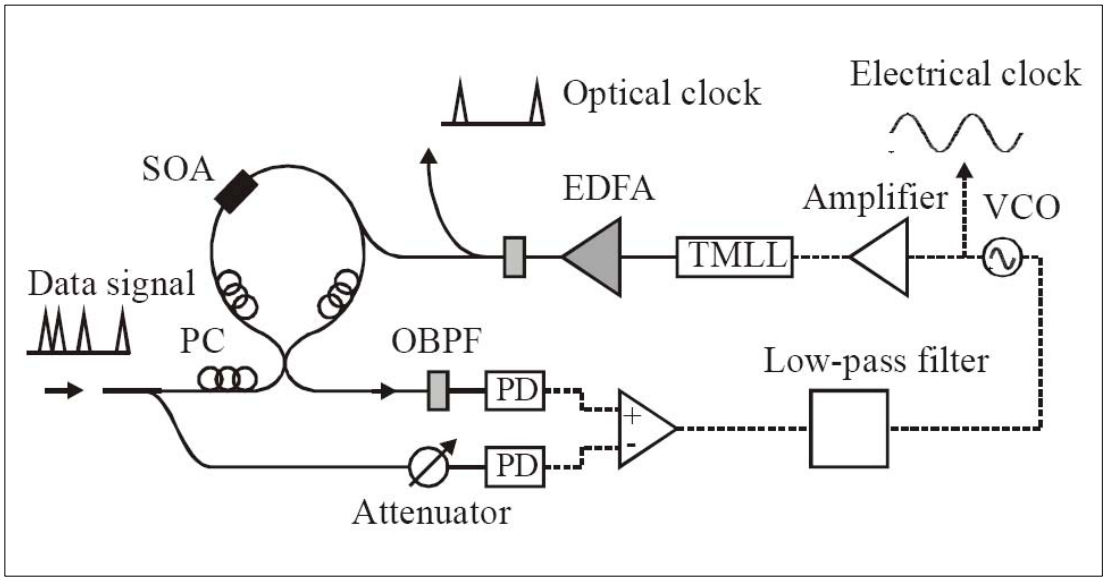

Figure 3.13 Optical clock recovery using an opto-electronic phase locked loop and interferometric SOA switch, PD: photodiode, TMLL: tuneable mode locked laser, OBPF: optical bandpass filter, PC: polarisation controller, VCO: voltage controlled oscillator.

In OTDM systems, clock recovery is required in optical receivers and in 3R regenerators. At high speeds clock recovery is best achieved using an optical solution. An SOA technique (Figure 3.13) uses a phase locked loop with an SOA based interferometric switch. In this configuration the OTDM data signal is coupled to the SOA loop mirror, which is driven by an optical control pulse train generated by a tuneable mode locked laser (TMLL), whose repetition frequency is determined by a voltage-controlled oscillator (VCO). The output signal from the loop mirror is detected by a slow photodiode. A fraction of the input signal is switched from the loop mirror at the repetition rate of the control pulses. When the VCO frequency is equal to the base frequency of the input signal, the switched components of the input signal have constant phase within a time slot. In this case the output signal from the photodiode becomes a DC signal whose amplitude is proportional to the phase difference between the input signal pulses and control pulse train, i.e. the optical switch acts as a phase comparator. However this error signal only has a single polarity so there is no discrimination between negative and positive phase differences. This problem can be overcome by detecting the signal using a second slow photodiode. The output signal from this photodiode is subtracted from the error signal. The resulting signal is sent to the VCO via a low-pass filter. This closes the loop and locks the VCO frequency to the base frequency of the input data signal. The optical clock pulses can then be extracted from the output of the TMLL using a coupler (Connelly, 2002).

3.6 SOA's Future

SOA technology is capable of realising many of the all-optical functions required in emerging optical networks. As optoelectronic integrated circuit technology advances and manufacturing costs fall, the use of SOAs as basic amplifiers and as components in functional subsystems will expand.

CHAPTER FOUR
TRANSMISSION LINE MATRIX METHOD (TLMM)

4.1 Introduction

Before the advent of powerful digital computers, complicated electromagnetic problems which do not have analytical solution could only be solved by simulation techniques. When modern computers became available, powerful numerical techniques could be used to predict directly the behavior of the field quantities. The great majority of these methods results in harmonic solutions of Maxwell's equations in the space or spectral domain. The transmission-line matrix (TLM) method of analysis represents a true computer simulation of wave propagation in the time domain.

4.2 Discretization of Wave Equations

According to Huygens principle, a wavefront consists of a number of secondary radiators which give rise to spherical wavelets. The envelope of these wavelets forms a new wavefront which gives rise to a new set of spherical wavelets, and so on. Because the difficulties in the mathematical formulation of this mechanism, its application does not lead to an accurate description of wave propagation and scattering (Saleh, 1991).

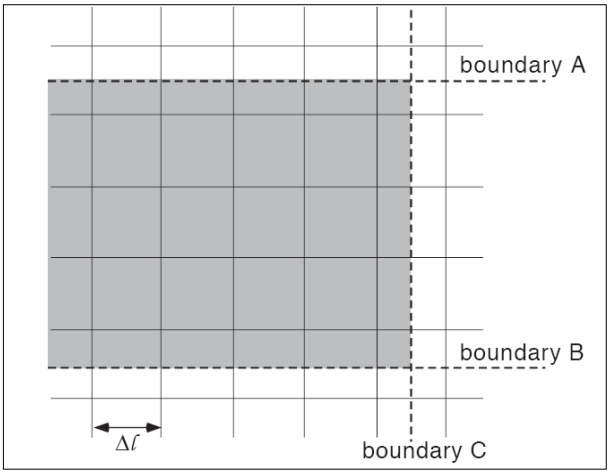

Figure 4.1 Schematic network

In order to implement Huygens's model on a digital computer, we must formulate it in discretized form (Figure 4.1). Both space and time are represented in terms of finite, elementary units Δl and Δt, which are related by the velocity of light such that

$$\Delta t = \Delta l / c.$$

Two-dimensional space is modeled by a Cartesian matrix of points or nodes, separated by the mesh parameter Δl. The unit time Δt is then the time required for an electromagnetic pulse to travel from one node to the next.

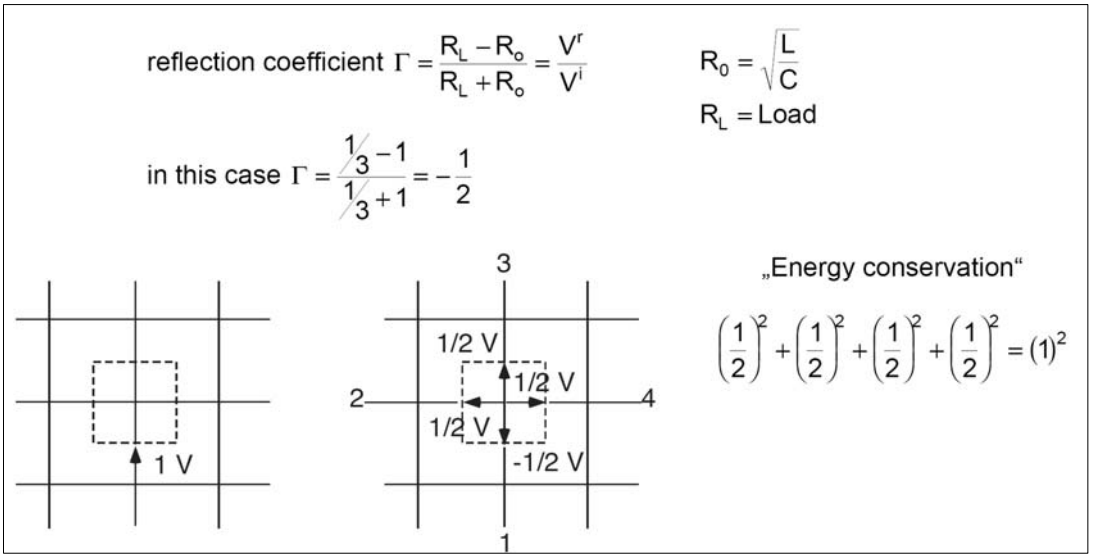

Figure 4.2 The impulse response of a node in a scattering matrix

Assume that a delta function impulse is incident upon one of the nodes from the negative x-direction (Figure 4.2). The energy in the pulse is unity. In accordance with Huygen's principle, this energy is scattered isotropically in all four directions, each radiated pulse carrying ¼ of the incident energy. The corresponding field quantities must then be ½ in magnitude. The reflection coefficient "seen" by the incident pulse must be negative in order to satisfy the requirement of field continuity at the node (Hoefer, 1985).

The incidence of a unit Dirac voltage-impulse on a node in the TLM mesh is seen in the Figure 4.2. Since all four branches have the same characteristic impedance, the

reflection coefficient “seen” by the incident impulse is indeed -½, resulting in a reflected impulse of -0.5 V and three transmitted impulses of +0.5V.

The more general case of four impulses being incident on the four branches of a node and they can be obtained by superposition from the previous case. If at time $t = k\Delta t$, voltage impulses ${}_kV_1^i, {}_kV_2^i, {}_kV_3^i$ and ${}_kV_4^i$ are incident on lines 1, 2, 3 and 4 then the total voltage impulse reflected along line n at time $t = (k+1)\Delta t$ on any junction node, will be

$$ {}_{k+1}V_n^r = \frac{1}{2}\left[\sum_{m=1}^{4} {}_kV_m^i\right] - {}_kV_n^i $$

This situation is described by a scattering matrix equation relating the reflected voltages at time $t = (k+1)\Delta t$ to the incident voltages at the previous time step $k\Delta t$.

$$ {}_{k+1}\begin{bmatrix} V_1 \\ V_2 \\ V_3 \\ V_4 \end{bmatrix}^r = \frac{1}{2}\begin{bmatrix} -1 & 1 & 1 & 1 \\ 1 & -1 & 1 & 1 \\ 1 & 1 & -1 & 1 \\ 1 & 1 & 1 & -1 \end{bmatrix} \times {}_k\begin{bmatrix} V_1 \\ V_2 \\ V_3 \\ V_4 \end{bmatrix}^i $$

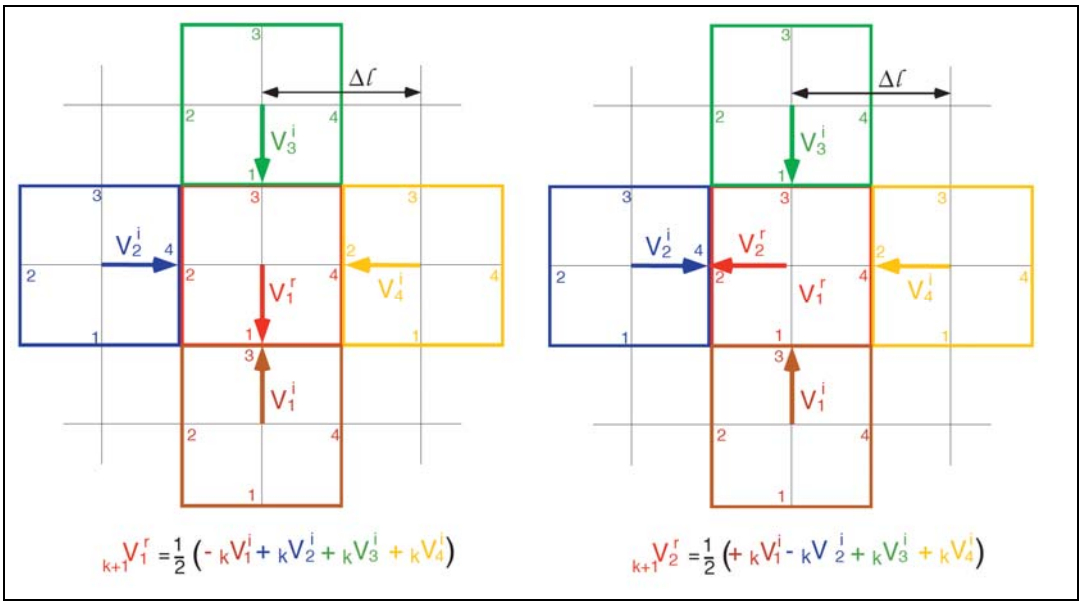

Figure 4.3 How to get V^r out of V^i.

Any impulse emerging from a node at position (z, x) in the mesh (reflected impulse) becomes automatically an incident impulse on the neighboring node. Hence,

$$_{k+1}V_1^i(z, x + \Delta l) = {}_{k+1}V_3^r(z, x)$$
$$_{k+1}V_2^i(z + \Delta l, x) = {}_{k+1}V_4^r(z, x)$$
$$_{k+1}V_1^i(z, x - \Delta l) = {}_{k+1}V_1^r(z, x)$$
$$_{k+1}V_1^i(z - \Delta l, x) = {}_{k+1}V_2^r(z, x)$$

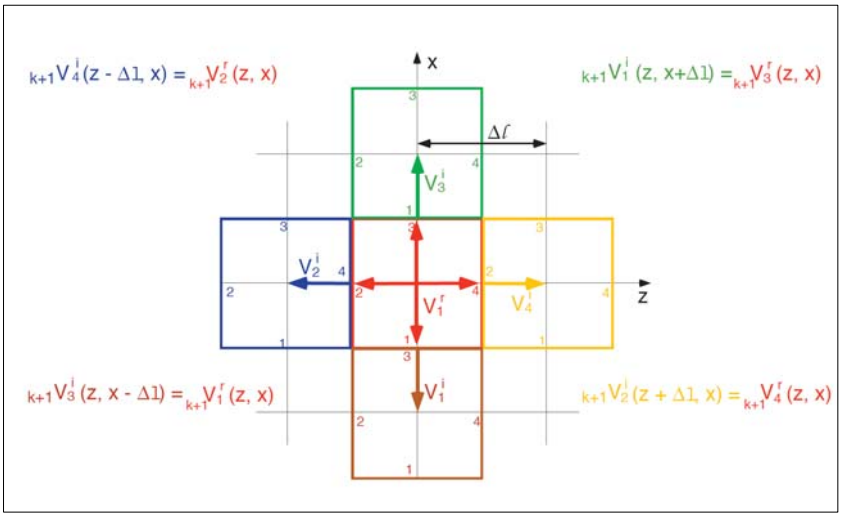

Figure 4.4 How to get V^i out of V^r.

If the magnitudes, positions, and directions of all impulses are known at time $t = k\Delta t$, the corresponding values at time $t = (k + 1)\Delta t$ can be obtained by operating the equations above on each node in the network. The impulse response of the network is then found by initially fixing the magnitudes, directions, and positions of all impulses at $t = 0$ and then calculating the state of the network at successive time intervals (Johns, 1971).

The scattering process described above forms the basic algorithm of the TLM method. Three consecutive scattering are shown in Figure 4.5, visualizing the spreading of the injected energy across the two-dimensional network. This sequence of events closely resembles the disturbance of a pond due to a falling drop of water. However, there is one obvious difference, namely the discrete falling drop of water. However, there is one obvious difference, namely the discrete nature of the TLM

mesh which causes dispersion of the velocity of the wavefront. In other words, the velocity of a signal component in the mesh depends on its direction of propagation as well as on its frequency. Harmonic solutions to a problem are obtained from the impulse response via the Fourier transform. Accurate solutions will be obtained only at frequencies for which the dispersion effect can be neglected.

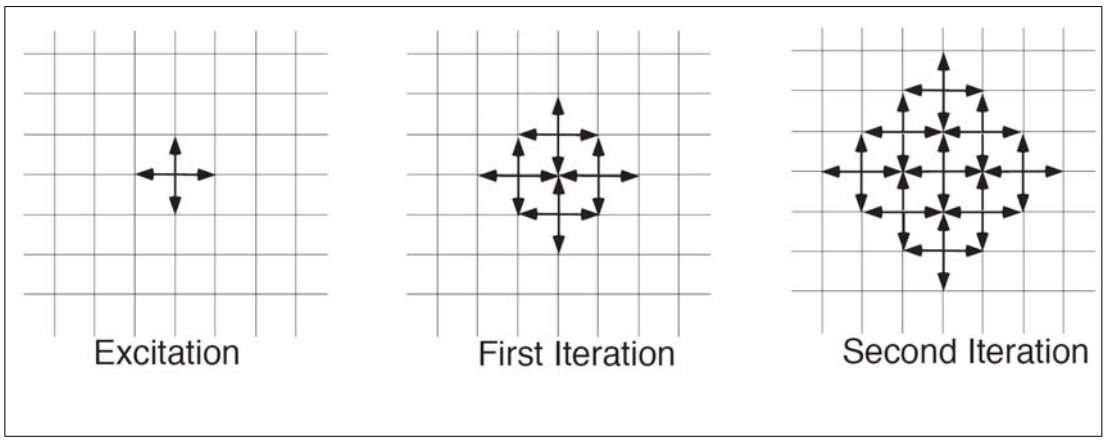

Figure 4.5 Iterations of TLM

The TLM mesh can be extended to three dimensions, leading to a rather complex network containing series as well as shunt nodes. Each of the six field components is simulated by a voltage or a current in that mesh (Hoefer, 1985).

4.3 Wave Properties of TLM

TLM model has a network analog in the form of a mesh of orthogonal transmission lines, or transmission-line matrix, forming a Cartesian array of shunt nodes which have the same scattering properties as the nodes in Figure 4.6. It can be shown that there is a direct equivalence between the voltages and currents on the line mesh and the electric and magnetic fields of Maxwell's equations.

The basic building block of a two-dimensional TLM network is a shunt node with four sections of transmission lines of length $\Delta l/2$ (Figure 4.6). Such a configuration can be approximated by the lumped-element model shown in Figure 4.6. Comparing the relations between voltages and currents in the equivalent circuit

with the relations between the H_z-, H_x-, and E_y- components of a TE_{m0} wave in a rectangular waveguide, the following equivalences can be established:

$$E_y \equiv V_y \qquad -H_z \equiv (I_{x3} - I_{x1})$$
$$-H_x \equiv (I_{z2} - I_{z4}) \qquad \mu \equiv L \qquad \varepsilon \equiv 2C$$

For elementary transmission lines in the TLM network, and for $\mu_r = \varepsilon_r = 1$, the inductance and capacitance per unit length are related by

$$\frac{1}{\sqrt{LC}} = \frac{1}{\sqrt{\mu_0 \varepsilon_0}} = c$$

where $c=3 \times 10^8$ *m/s*.

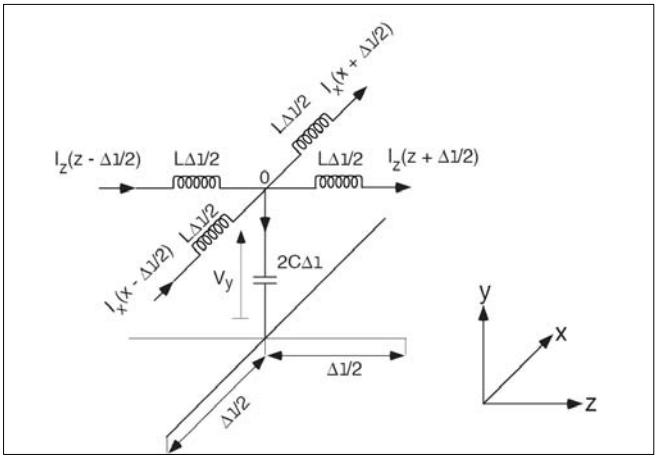

Figure 4.6 The basic building block of two dimensional TLM.

If voltage and current waves on each transmission-line component travel at the speed of light, the complete network of intersecting transmission lines represents a medium of relative permittivity twice that of free space. As long as the equivalent circuit in Figure 4.6 is valid, the propagation velocity in the TLM mesh is $1/\sqrt{2}$ the velocity of light (Johns, 1972).

4.4 Transmission Line Laser Model (TLLM)

Transmission-line laser models allow the full dynamics of semiconductor lasers and semiconductor amplifiers to be efficiently simulated, including the spectral

dynamics. Because a TLLM is a close representation of the laser, a single standard model is able to predict:

- nonlinearities during analog modulation
- evolution of lasing spectra during modulation
- CW spectral performance and purity (multimode, single-mode, noise…)
- spectra during modulation (mode-hopping, dynamic chirp, instabilities...)
- optical noise (intensity noise spectra, amplified spontaneous emission...)
- RF noise (relative intensity noise, excess noise due to feedback, chaos...)
- effects of external optical components, optical injection...
- modulation responses (IM, FM, magnitude and phase)
- linewidth

An individual TLLM is able to simulate Fabry-Perot and DFB lasers, and also Semiconductor Optical Amplifiers (SOAs). By interconnecting a TLLM with external components, or other TLLMs, the following devices and phenomena can be simulated. The devices include:

- external cavity lasers with diffraction gratings and etalons
- external cavity lasers using fiber Bragg gratings
- mode-locked lasers (integrated and external cavity, passive/hybrid/active)
- multi-section lasers (different materials and injection currents)
- tunable lasers (except transverse guide)
- optical gates, amplifiers, switches, regenerators and wavelength converters
- coupled lasers, for example in laser arrays
- optical preamplifiers (SOAs)
- almost all optical circuits and systems

The phenomena include:

- effects of unwanted optical feedback including chaos, mode-hopping
- effects of optical injection into a laser for stabilization
- optical switching in Sagnac loops
- transmission of analog and digital signals including noise phenomena

- millimeter-wave signal generation using mixing of multiple lasers

The simulations in the next two chapters give some applications of TLLM.

4.5 Transmission Line Laser Modeling Basics

Transmission-Line Laser modeling (TLLM) is a technique for developing numerical algorithms for laser and semiconductor amplifier simulation. TLLM is based on the algorithm design methods introduced by Johns and Beurle in their Transmission-Line Matrix (TLM) method of simulating microwave cavities in the time-domain by using meshes of transmission-lines. TLLM offers unconditionally stable numerical algorithms, and because they are based on a physical network, the approximations necessary for converting a continuous system to a discrete numerical model, are fully defined and understood. TLLM is as a way of defining a digital filter representation for the laser, where the topology of the filter closely simulates the physical structure of the laser cavity (VPI Photonics, 2004).

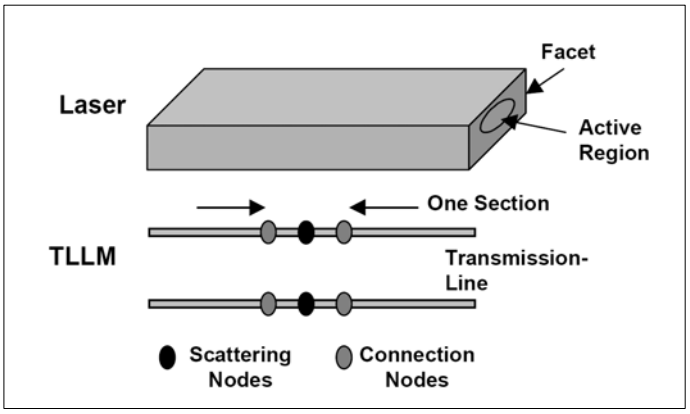

Figure 4.7 Schematic of a semiconductor laser and its TLLM

In TLLM, the laser is divided into longitudinal sections, as shown in Figure 4.7. Each section contains scattering nodes representing the gain (stimulated emission), loss (scattering and absorption), and noise (spontaneous emission) that optical waves experience while passing through the section. The nodes of adjacent sections are connected by transmission-lines. These transmission-lines represent the waveguide propagation delay. Samples of the optical (electric) field are passed between the

nodes on these transmission lines. In the simplest of lasers, the pulses are unmodified as they pass from node to node, through the connection matrices, thus the transmission lines are distortion-less, and are simply represented as memory locations in the computer.

The advantages of thinking of the model as being an electrical circuit equivalent of the laser rather than a set of equations based on the physics of the laser (and both ways of thinking are valid) are:

- that transmission-line theory can be applied in the model to speed its solution
- that any approximations in the model are represented by parasitic elements in the equivalent circuit. Thus, it is easy to visualize the effects of approximations and to judge their importance
- that the parasitics (hence approximations) can generally be reduced by decreasing the timestep (sampling interval)
- that transmission-lines translate easily into fixed delays (usually one iteration) in the algorithm.

For convenience all the transmission-lines have an equal delay, which is called the time step of the model. This time step is simply the distance between the nodes divided by the average group velocity of light in the waveguide. The iteration process comprises of repeated scattering then connecting (VPI, 2004).

4.6 Scattering

Scattering comprises generating reflected forward and backward optical waves at each node, from incident forward and backward waves. The scattering matrix represents the optical processes of stimulated emission, absorption, and spontaneous emission, and coupling due to the Bragg grating in DFB lasers. Figure 4.8 shows the position of optical pulses before and after scattering.

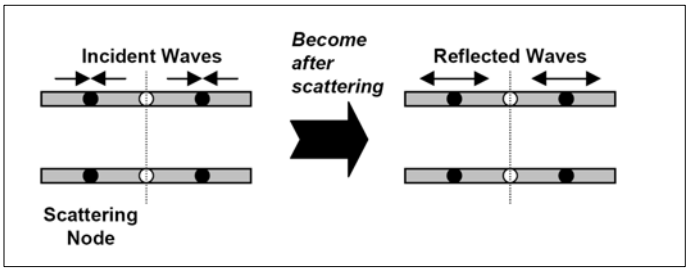

Figure 4.8 Scattering at a scattering node.

4.7 Connecting

Connecting comprises propagating these reflected waves to the adjacent nodes where they become incident waves again, to be operated on by the next scattering process. Connecting implies propagation along the transmission lines, which have one time step delay. Figure 4.9 shows the position of optical pulses before and after scattering. The output of the model is therefore a stream of optical field samples separated by the model time step. Usually these samples are taken from the end of the laser cavity, as in reality. The optical spectrum can be easily calculated by taking a Fourier transform of these samples.

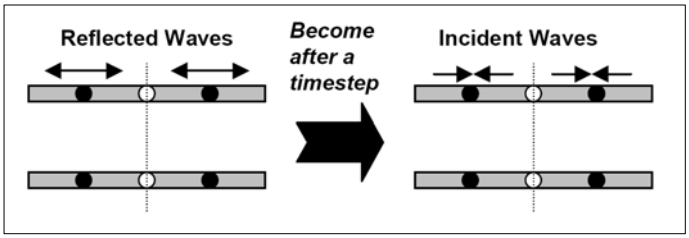

Figure 4.9 Connecting between model sections

4.8 SOA Modeling

Semiconductor optical amplifiers are simply Fabry-Perot lasers with anti-reflection coated facets, and an optical input to one of the facets. The addition of anti-reflection coated facets and simply redefining the parameters is all that is needed. The optical input can either come from another device model or a variety of optical signal generators. The noise and signal behavior are easily modeled, as are the switching dynamics of amplifiers with reflective facets. Note that the gain across

a section is relatively large in an amplifier, compared with the gain required to maintain oscillation in a laser. Unlike other algorithms, the TLLM algorithm models the magnitude of gain exactly at the peak of the gain curve so that SOAs will give the correct overall gain.

CHAPTER FIVE
A NOVEL ALL-OPTICAL ROUTING ARCHITECTURE FOR OPTICAL PACKET SWITCHED NETWORKS

5.1 Introduction

In this work, a novel all-optical routing architecture (Mocan, 2006) based on available optical techniques and devices, is proposed. The design relies upon self-routing of the optical data packets using the packet's address information and the routing table of the network topology. Network protocols with smaller and simpler routing tables have high potential to accommodate this design. Especially latest, popular network protocols such as Multi Protocol Label Switching (MPLS) and Internet Protocol version six (IPv6) data packets might be very efficiently routed by this technique.

IPv6 has much larger address space (128 bits) than IPv4 (32 bits), which enables the use of multiple levels of hierarchy inside the address space. Each level helps to aggregate its IP space and enhance the allocation function. Service providers and organizations may have a tiered hierarchy (Desmeu, 2003). It means there are fewer routes to analyze, fewer fields to process, and fewer decisions to make in forwarding a data packet (Davies, 2003).

MPLS is another forwarding technique in autonomous networks that may accommodate this approach for optimizing the routing process (Tomsu & Schmutzer, 2002). Global network reachability is handled at the edge and packet forwarding rules are propagated to the core network. Label Edge Routers (LER) work as interface between the MPLS network and IP Internet and assign simple labels for the incoming packet streams. A MPLS network consists of Label Switch Routers (LSR) in the core of the network. Within the MPLS network, traffic is forwarded via LSRs just using the labels. MPLS and IPv6 are designed to improve the routing and switching bottlenecks of the current Internet Protocol (IPv4). Therefore, the novel

routing architecture proposed here might be adapted for both IPv6 and MPLS networks (Tomsu & Schmutzer, 2002).

Optical buffers, optical switches, header recognition, and route decision units are key building blocks of a general optical routing node. Truly photonic routers require photonic implementations of all these functions. The lack of all-optical processors and random access memories force designers to implement specific signal processing algorithms in separate optical modules. However, the interactions among these models should be carefully considered to overcome the synchronization and stability problems that may arise on ultra-fast data rates. The use of fixed length packets can, however, significantly simplify the implementation of packet content resolution and buffering as well as packet synchronization (Dinleyici & Mocan, 2002), (Mocan & Dinleyici, 2003).

5.2 Operation Principle

The proposed all-optical routing architecture consists of a number of optical signal processing blocks as shown in Figure 6.1. At the input, only a small part of the incoming signal's energy is taken by a Y-coupler for processing to generate the routing information.

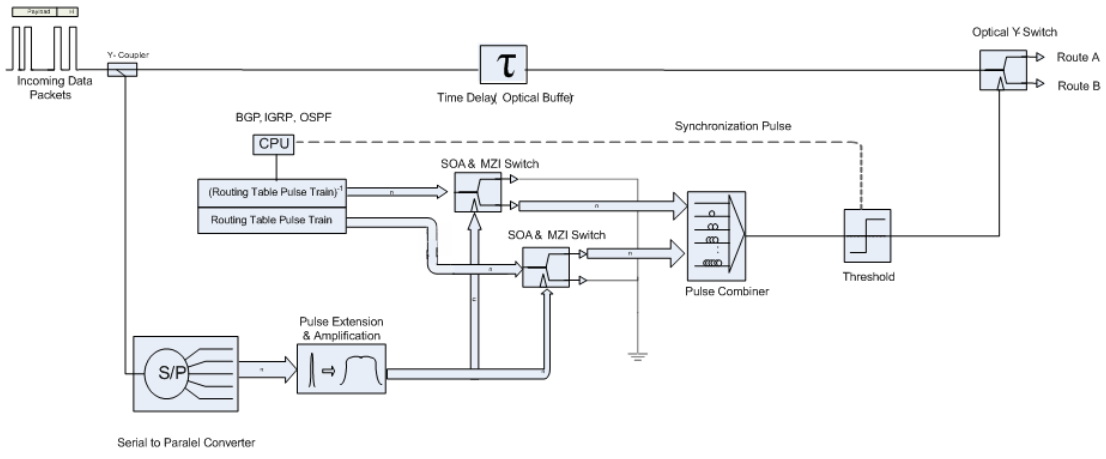

Figure 5.1 Novel All-Optical Router Architecture

The first step of the operation is header recognition and serial to parallel conversion of the header bits. Various techniques might be applied for these operations (Cotter, 1995), (Boyraz, 2003), (Takahashi, 2001). Every serial-to-parallel converted bit is sent to the pulse extension module, which extends the pulses in time up to the duration of the whole addresses in the routing table. Pulse extension operation makes each address bit available for the exclusive-or (XOR) operation between the entire pulse train of the routing table. The length of the routing table strongly affects the duration of the algorithm, and this limitation may be overcome by increasing the generation speed of the routing table.

The routing table pulse train (RTPT) might be generated by an ultra-fast pulse generator, which is driven by an ordinary CPU. The use of an electronic CPU may not cause a delay in routing, because it is only used to keep the routing tables updated, which is a very slow process (30-120 sec) compared to the packet bit rates (Gbps). RTPT, which includes "Route A" addresses, and its logical inverse $RTPT^{-1}$ are required for the special all-optical XOR algorithm. If an address header carries the logic "1" information, the result of the XOR operation between RTPT and address bit is the RTPT itself, and if the address header has the logic "0" information the XOR operation results in $RTPT^{-1}$. As a result, only a switching operation between RTPT and $RTPT^{-1}$ that depends on the value of the address bits is sufficient to achieve an optical XOR operation.

Using this useful trick an all-optical XOR is realized, which uses a counter propagating semiconductor optical amplifier assisted Mach-Zehnder interferometer (SOA-MZI) switch (Tajima, 2003). In this case, the extended address bits are used as control signals while RTPT and $RTPT^{-1}$ are input signals. When the routing table contains the address of the incoming packet a series of optical 1's are produced consecutively at the XOR outputs. The XOR outputs are combined by synchronization delays and pulse combiners and passed through a suitable threshold element to generate the routing control bit that triggers the optical switch at the output port. According to the state of the routing control bit, the data packet is switched to either "Route A" or "Route B" as default. During the routing decision

time interval the original data packet is kept in the optical buffer, which may be designed of fixed length fiberoptic cable, because of static delay line requirement.

All-optical routing of 12-bit fixed sized packets having 3-bit address headers is simulated using the novel routing technique proposed here. “VPI Photonics VPI Transmission Maker 6.5” simulation software is used as the simulation environment. It delivers verified models of common optical devices and it is easy to construct new ones by using the design tools of the software. Optical pulse generators, modulators, couplers, delay elements, interferometers, pulse combiners, optical switches, fiber Bragg grating filters, fiber amplifiers, bulk semiconductor amplifiers, and many other optical devices are already available within the software. But optical devices like the optical threshold element and the SOA-MZI switch with backward propagation, which are not included in the software have been designed using signal processing tools or combination of the current models.

5.3 Threshold Element

The threshold device can be realized by the combination of two different periodically layered materials with refractive indices of opposite sign (Brzozowski, 2000). The refractive index of a single layer is the function of the light intensity I, linear index coefficient n_0 and the nonlinear Kerr coefficient n_{nl}.

$$n = n_0 + n_{nl} I$$

The Bragg condition of a linear periodic structure for a medium with intensity dependent refractive indexes could be expressed as (Brzozowski, 2000):

$$(n_{01} + n_{nl1} I) d_1 + (n_{02} + n_{nl2} I) d_2 = \frac{\lambda}{2}$$

The Bragg condition is used to determine the spectral position ‘λ’ of the center of the periodic grating. A stable stop-band, which stays fixed in an intensity

dependent medium, could be satisfied if and only the Kerr-coefficients have opposite signs. Required thickness (d_1 and d_2) for the chosen material set could be determined in terms of linear and nonlinear refractive indexes (Brzozowski, 2000), (Brzozowski, 2001).

The variation of the intensity and refractive index for different values of I_{in} across the grating period of 1000 has been experimented by Brzozowski with material parameters:

$$n_{01} = 1.5,\ n_{02} = 1.52,\ n_{nl1} = 0.01 \text{ and } n_{nl2} = -0.01.$$

The threshold parameter "a" is defined as:

$$a = (n_{01} - n_{02}) \big/ (|n_{nl1}| + |n_{nl2}|)$$

for the given material pairs.

Low incident intensity ($I_{in} = 0.3$) is blocked by the grating profile and decays sharply to a negligible intensity level. As the intensity increases closer to a the refractive index variation helps to reflect the incident intensity across the structure (for $I_{in} = 0.65$). When the incident intensity is equal to a the grating profile will be terminated by the refractive index change and the incident intensity is transmitted completely. As the incident intensity is increased above a (e.g., $I_{in} = 1.07$) the grating will be formed again and forces the intensity to be normalized. The approximate piecewise-linear relation between transmitted and incident intensity is as given below (Brzozowski, 2001);

$$I_{out} = \begin{cases} 0 & for \quad I_{in} < a(1 - 1/2^N) \\ a[2^N (I_{in} - 1) + 1] & for \quad a(1 - 1/2^N) < I_{in} < a \\ a & for \quad I_{in} > a \end{cases}$$

A threshold device will be in transmit state for inputs greater than or equal to threshold value "a", and the otherwise will be zero as shown in Figure 5.2.

Furthermore, arranging the proposed structure in series results in increasingly steep transition characteristics.

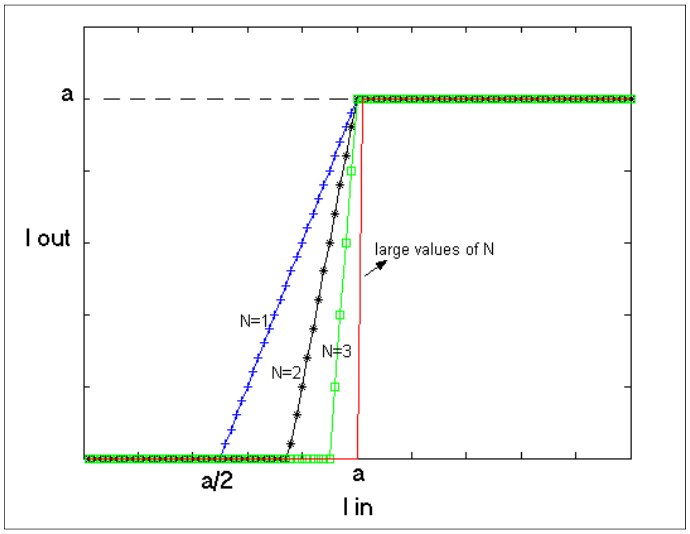

Figure 5.2 Intensity variation for a N-layer grating structure.

The fast response of the molecular reorientation makes the Kerr-effect a prime candidate for the use in quick optical gate or optical hard-limiter. In addition, it helps to remove some spikes and noises and normalizes the output. Using the mathematical model in References (Brzozowski, 2000) and (Brzozowski, 2001) the threshold device is designed and simulated in Virtual Photonics simulation software. It is used at the various points of the architecture for different threshold levels.

5.4 Pulse Extension

An important step of the algorithm is the extension of the parallel address bits in the time domain. The aim of the pulse extension is to prepare the header information bits for the XOR operation with the routing table pulse train. The routing table is set up as a sequence of pulse trains, which includes all address bits in serial form. In the routing decision procedure, the whole routing table and the each extended address bit have to be XORed together. The uniform Bragg grating filtering method is used to extend the pulse up to the desired duration. The pulse, which is chosen Gaussian, is dispersed in the time domain by adjusting the filter bandwidth and the filter order. Signal amplification is needed as well because of the power lost during the extension step.

A fiber Bragg grating is a periodic perturbation of the refractive index (n_{eff}) along the fiber length (Mocan & Dinleyici, 2003), which in general can be described as (Hill & Melz, 1997):

$$\delta_{neff}(z) = \bar{\delta}_n(z)\left(1+\upsilon\cos\left[\frac{2\pi}{\Lambda}z+\phi(z)\right]\right)$$

where $\delta_n(z)$ is the "dc" index change spatially averaged over a grating period, υ is the fringe visibility of the index change, Λ is the nominal period defining filter center frequency and $\phi(z)$ describes the grating chirp. In a uniform filter we used, the refractive index $\delta_n(z)$ and $\phi(z)$ are constant. A transfer function of the uniform filters can be calculated analytically and is given by (Hill & Melz, 1997), (Erdogan, 2001):

$$T(f) = \frac{\kappa\sinh\sqrt{\kappa^2-\xi^2}}{\xi\sinh\sqrt{\kappa^2-\xi^2}+j\sqrt{\kappa^2-\xi^2}\cosh\sqrt{\kappa^2-\xi^2}}$$

κ describes the coupling "strength" between the incident and reflected waves (E_{in} and E_{out}) and parameter ξ represents a normalized frequency offset from the center-frequency of the filter. κ can be found from the maximum FBG reflectivity $R_{\max} = |E_r / E_i|^2$ according to $\kappa = \tanh^{-1}\sqrt{R_{\max}}$ and is defined by the FBG length L and the refractive index perturbation as given by $\kappa = (\pi/\lambda)\delta_{neff}L$, where λ is the wavelength of the light wave (Hill & Melz, 1997), (Erdogan, 2001).

A uniform fiber Bragg grating filter with the transfer function of $T(f)$ is used to extend the Gaussian optical pulses with peak pulse power of 1 mW and 0.1 ns pulse width. Simulation results (Mocan & Dinleyici, 2002) include pulse extension and amplification (≈15 dB) of the 0.1 ns pulses up to the 3.2 ns as shown in Figure 5.3.

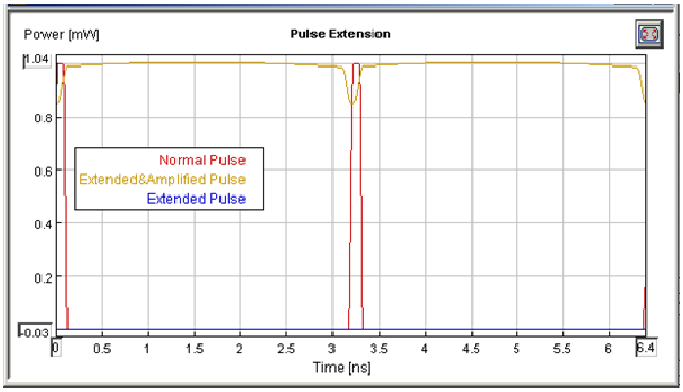

Figure 5.3 Extension and amplification of a 0.1 ns optical pulse.

The simulation parameters are as given below:

$$R_{max} = 0.95, \quad \kappa = 2.17827, \quad \Delta f_0 = 100 \text{ GHz}, \quad f_c = 0, \quad \lambda = 1.55 \text{ μm};$$
$$\Lambda = 0.531 \text{ μm}, \quad \nu = 1, \quad \delta_n = 0.0004, \quad L = 2.68678 \text{ mm}.$$

The pulse energy efficiency of the pulse extension unit for the ideal Bragg grating extension filtering is calculated as ≈ 91.609% for 1-to-32 extension rate (Mocan & Dinleyici, 2002).

The pulse extension operation could be done by other alternative methods. Optical materials with longer relaxation times might be another solution to the problem. Triggering of this sort of optical materials or semiconductor laser diodes in on-off keying approach may be a solution, too.

5.5 All Optical XOR Operation

Another critical point of the design is the realization of the SOA assisted MZI switch (Tajima, 2003), which will be used as an all-optical XOR gate. The SOA-MZI switch realizes the XOR operation between two pulse streams, routing table pulse train, and parallel address bits. The optical SOA-MZI switch in our study consists of a symmetrical MZI and a bulk SOA with reverse inputs. Two input signals are fed to the XOR module bidirectionally to interfere at the bulk SOA. The semiconductor

amplifier based Mach-Zehnder interferometer posses the practical advantages of low power consumption, low latency, high stability, and integration potential (Tajima, 2003). Although, the simulation is performed for 10 Gb/s, the SOA-MZI has the potential to operate at 160 Gb/s or higher bit rates (Stobjaer, 2000). The parameters of the bulk SOA module of the *VPI VirtualPhotonics* are optimized through analysis and simulations.

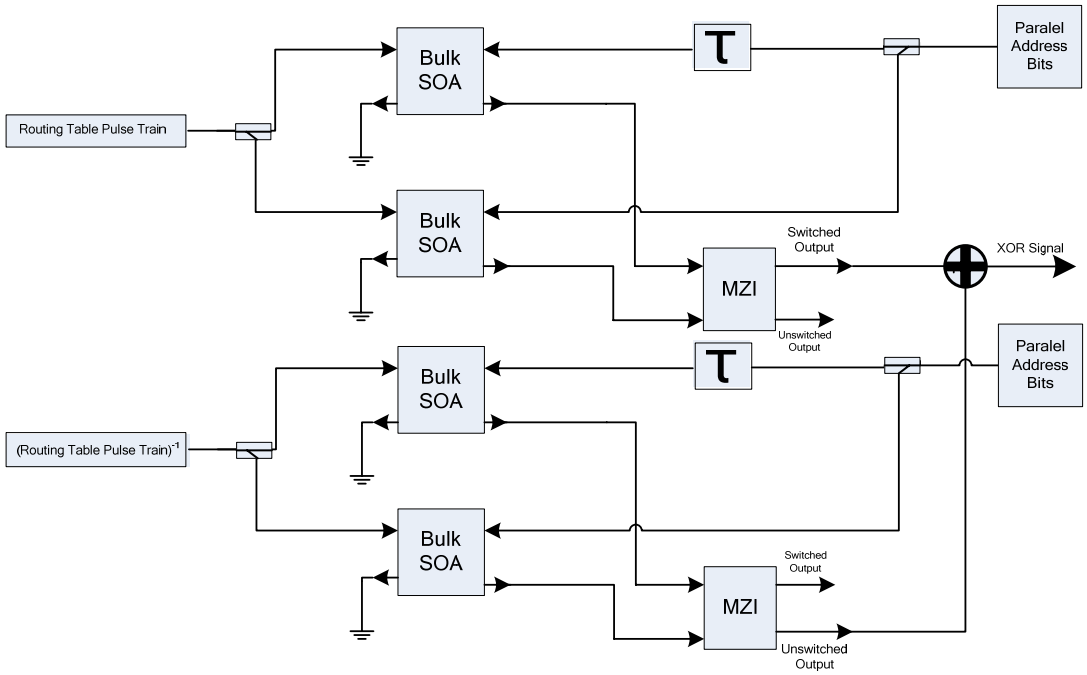

Figure 5.4 SOA-MZI switch for optical XOR operation

For the switching operation, the RTPT and its inverse $RTPT^{-1}$ enter to the inputs of the two identical bulk SOAs as probe signals. The header bits are functioning as the control signals and fed from the backward propagation input of the bulk SOAs. The parallel header bits are used to drive a clock sequence. When a header clock pulse enters the SOA, it stimulates the recombination of carriers as a response to stimulated amplification. The carrier density decreases sharply on each arrival of a pulse, and it recovers slowly until the next pulse arrives. The fall time is approximately equal to the width of the original pulse. The routing table signal pulse is split into two components and fed into the inputs of the identical bulk SOAs as

forward propagating waves. Either the routing table pulse train or its inverse is used as the probe signal at the SOA input.

Address header bits are backwardly propagated and used to modulate a π-phase shift inside the SOA. The optical phase shift of each component is adjusted by the nonlinear change in refractive index of the respective SOA, as shown in Figure 5.5. This shifting of phase is slightly delayed for one of the pulse trains. This delay time Δt is produced by the difference between the times of arrival of the control pulses at the respective SOAs. The two split signal components collide and interfere each other at the interferometer's output. The phase bias between the two components is adjusted such that the phase difference before t_0 and after $t_0 + \Delta t$ equals to π. The rise and fall times of the rectangularlike switching window are determined by the width of the control pulse. The width of the switching window is determined by delay time Δt (Tajima, 2003). Each pulse of the clock sequence produces a π (180°) phase shift on the probe signal and the MZI opens a near-rectangular switching window and thus gates the routing table pulse train to the switched port. If the header bit is zero, there is no phase shift or switching window on the pulses and there will be no significant signal power at the output.

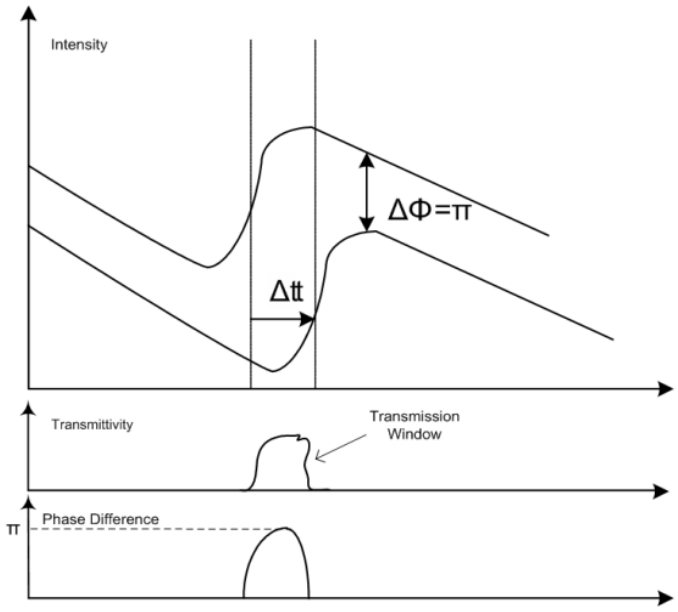

Figure 5.5 Nonlinear phase shift of SOA.

5.6 Simulation Results

The fixed length data packets having three bits of header are generated from On/Off keying modulated Gaussian pulses with 0.1 ns pulse width and 10 Gbps pulse repetition rate. According to the address information each packet will be sent to either “Route A” or “Route B”. In the following example the routing table includes the addresses 000-111-010-100 for “Route A”. For every one of these addresses, a routing control bit will be generated to set the optical switch at the output port. Routing table information signals RTPT and its logical inverse $RTPT^{-1}$ are readily stored in a memory unit and generated by an ultrafast pulse generator.

Table 5.1 Logical operation principle of the XOR for “101”

	XOR Operation of the Mismatching Address Bit “101”														
RTPT			0	0	0	1	1	1	0	1	0	1	0	0	0
$RTPT^{-1}$		1	1	1	0	0	0	1	0	1	0	1	1	1	
RTPT	0	0	0	1	1	1	0	1	0	1	0	0	0		
Synch.			↑			↑			↑			↑			
∑ Power			**1**	2	1	**2**	1	3	**0**	3	0	**2**	1		

Table 1 explains the logical operation principle of the routing process and the function of the RTPT, $RTPT^{-1}$, and synchronization signals. Here, the packet is chosen to carry address “101” and because this address is not in the routing table, the routing algorithm should not generate a routing control bit at all. However, the routing table may include the shifted versions of the packets addresses (00011***101***0100, 0001110***101***00) which may result in inter bit matching errors. A synchronization signal whose repetition rate is aligned with the address length has been used to select the right bit sequence. The algorithm selects RTPT for “1” address bits and $RTPT^{-1}$ for “0” address bits to accomplish an XOR operation. If the routing table includes the header address a three optic one’s will present consecutively after the XOR operation. Each bit sequence is delayed for one-bit duration from the previous sequence, then summed and passed through an appropriate threshold device to generate the routing control bit. As it can be seen from Table 1, two sets of high-energized pulses (3-pulse energy) have been observed

at the pulse combiner, but they should be ignored since they do not overlap with the synchronization pulses.

The simulation results for the “101” addressed packets are shown in Fig. 5. Every bit of the address is separated and converted from serial to parallel (Fig. 6a-d) and they all have been extended in time domain up to the RTPT duration using Fiber Bragg Grating filtering (Fig. 5.6.1 to 5.6.8). A threshold component, as explained in previous section, is used in order to pulse reshaping by reducing the pulse fluctuations and normalizing the pulse peak power to 1 mW at the SOA-MZI switch input.

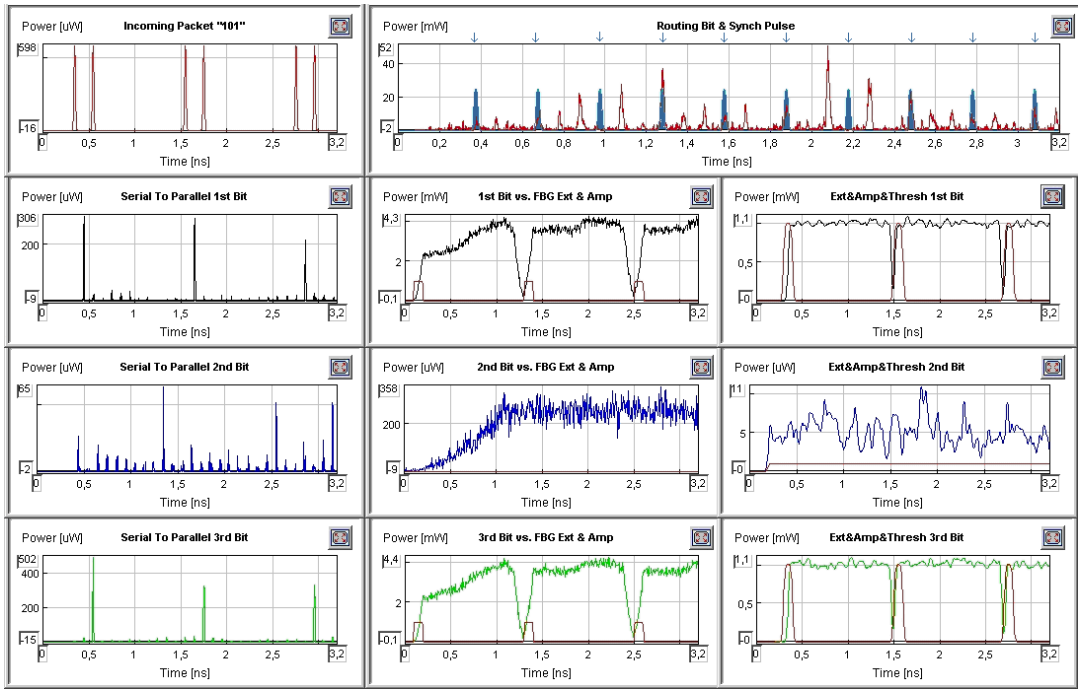

Figure 5.6. Simulation results for “101”

For the “0” bit the same operation results in low energized noise signals on the order of μW range, in contrast to the 1 mW for optical “1” pulses. Fig. 5.6.8 shows the resultant routing control signal and the synchronization pulses (dark pulses marked by arrows) as a result of the algorithm. As seen in the figure the high energized (~40 mW) pulses do not overlap with the synchronization pulses as expected. The sum of the routing control signal with the synchronization signal

should pass through a suitable threshold level for logical AND operation to set the optical switch at the output port. For “101”, the routing control bit is not generated and the packet is switched to “Route B” by default.

Table 5.2 Logical operation principle of the XOR for “000”

	XOR Operation of the Mismatching Address Bit “101”														
$RTPT^{-1}$			1	1	1	0	0	0	1	0	1	0	1	1	1
$RTPT^{-1}$		1	1	1	0	0	0	1	0	1	0	1	1	1	
$RTPT^{-1}$	1	1	1	0	0	0	1	0	1	0	1	1	1		
Synch.			↑			↑			↑			↑			
∑ Power			**3**	2	1	**0**	1	1	**2**	1	2	**2**	3		

Table 5.2 shows the logic table for the “000” addressed packets. Since the “000” address is in the routing table, the routing algorithm should produce a routing control bit to select “Route A”. Similarly, the routing control signal enables the $RTPT^{-1}$ after series of synchronization operations by following the routing procedure.

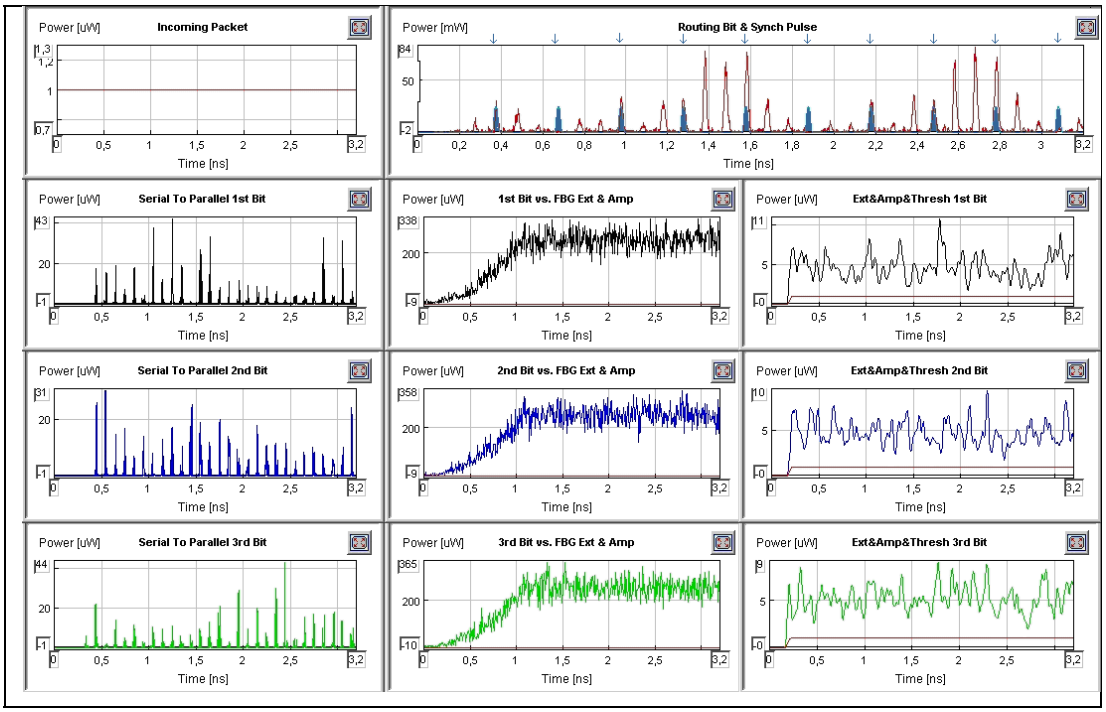

Figure 5.7 Simulation results for “000”

Figure 5.7 shows the simulation results for the “000” address. In Figure 5.7.2, there are three high energized pulses following each other. The synchronization pulses help us to discriminate the right set of the routing control signal. For the

packets with “000” addresses a routing control bit should be generated and the packet should be switched to “Route A” as happened in this case.

Table 5.3 Operation principle of the XOR for “111” and “001”

	XOR Operation of the Matching Address Bit “111”														
RTPT			0	0	0	1	1	1	0	1	0	1	0	0	0
RTPT		0	0	0	1	1	1	0	1	0	1	0	0	0	
RTPT	0	0	0	1	1	1	0	1	0	1	0	0	0		
Synch.			↑			↑			↑			↑			
∑ Power			**0**	1	2	**3**	2	2	**1**	2	1	**1**	0		
	XOR Operation of the Matching Address Bit “001”														
$RTPT^{-1}$			1	1	1	0	0	0	1	0	1	0	1	1	1
$RTPT^{-1}$		1	1	1	0	0	0	1	0	1	0	1	1	1	
RTPT	0	0	0	1	1	1	0	1	0	1	0	0	0		
Synch.			↑			↑			↑			↑			
∑ Power			**2**	3	2	**1**	0	2	**1**	2	1	**1**	2		

In the third case, packets with two different addresses are sent to the optical routing node. The first packet is carries the address “111” and the second one has address “001”. Table 5.3 shows that the first one should be routed to “Route A” and the second one should be routed to “Route B”.

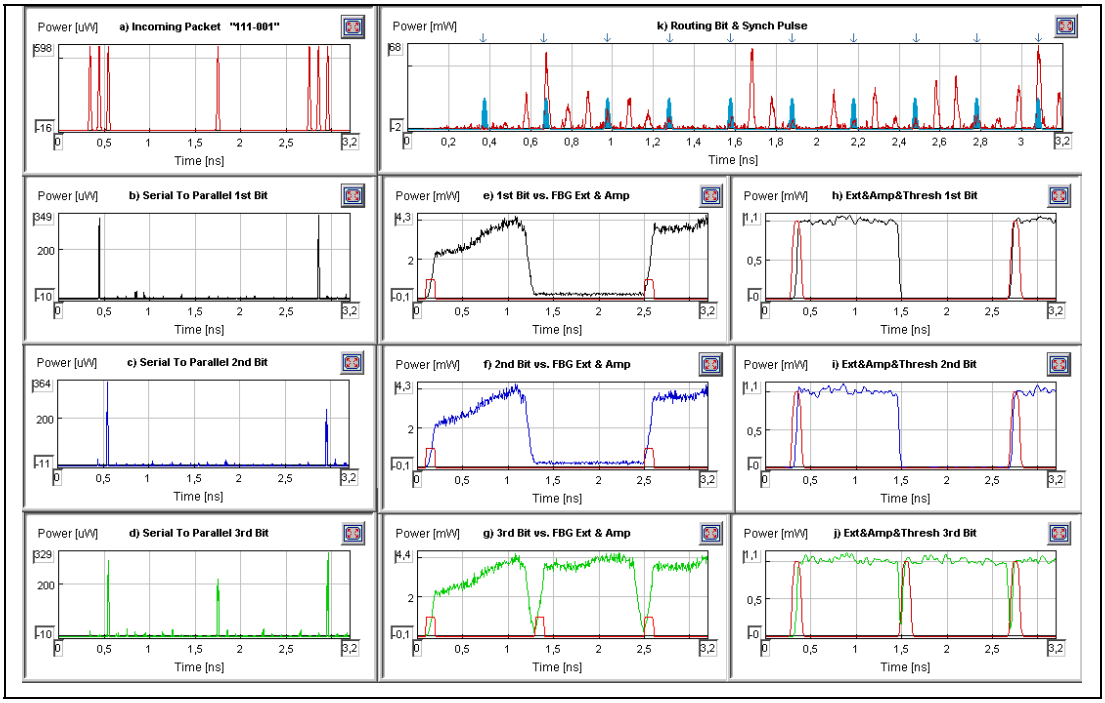

Figure 5.8 Simulation results for “111” and “001”

The simulation results (Mocan, 2006) in Fig. 5.8 shows that the control bit is generated at t = 0.7 ns for the first packet and as expected there is, however, no routing control bit produced for the second packet.

CHAPTER SIX
NOISE AND JITTER ANALYSIS OF THE CRITICAL COMPONENTS

6.1 Introduction

Previous chapter includes simulation results of whole all-optical routing node for packet switched networks. Some of the devices were modeled mathematically based on their features and characteristics. Noise, jitter, process delay and some other material properties were not analyzed in depth. In this chapter we will focus on nonideal cases and test the critical components by changing some of their parameters. The effects of numerical analysis method, bit rate, input laser power, bias current, switching window, carrier density, noise and jitter will be analyzed in detail.

Semiconductor Optical Amplifier(SOA) is the key component of the architecture. SOA's has been demonstrated successfully as optical switches, threshold elements, multiplexers and some logic elements. These devices are likely to be used widely in optical switching nodes because of their ultra fast switching abilities for both wavelength-division multiplexing (WDM) and optical time-division multiplexing (OTDM) applications. The integrability of several devices on the same substrate made them promising for the possible reduction of the functional node complexity. The simulations on this chapter will be focused on SOA's.

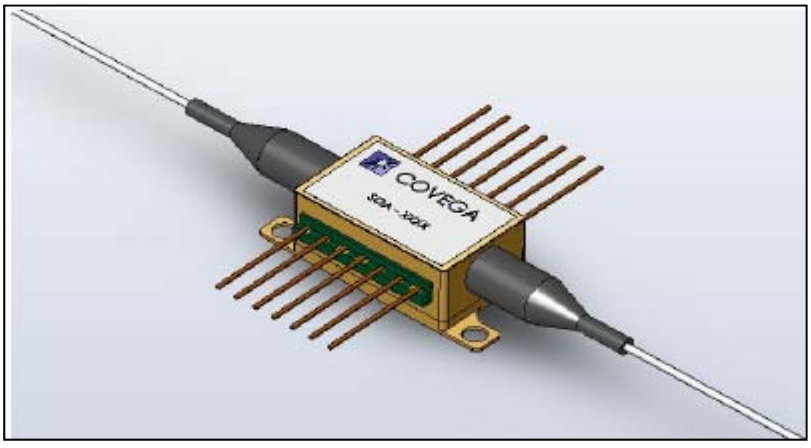

Figure 6.1 COVEGA's Nonliear SOA 1117

The real paramaters of Nonlinear SOA 1117: 1550 nm from COVEGA is used for the SOA model in the simulations. COVEGA's 1117 SOA is a polarization insensitive optical amplifier housed in a standard 14-pin butterfly package. Optoelectronic packaging techniques enable high output saturation power, low noise figure and large gain across a broad spectral bandwidth. This semiconductor is widely used in the industry for the nonlinear applications as 2R / 3R regeneration, four wave mixing and wavelength conversion. It has high fiber to fiber gain, broad spectral width and it is optimized for nonlinear applications.

6.2 Analysis of Simulation Method

TLLM (Transmission Line Laser Model) is used in numerical calculations for the laser rate equations. The method has been explained in chapter 4 of this thesis. A TLLM numerical model solution and analytical laser rate equation is compared both in spectral and time domain for two different sets of bit rate.

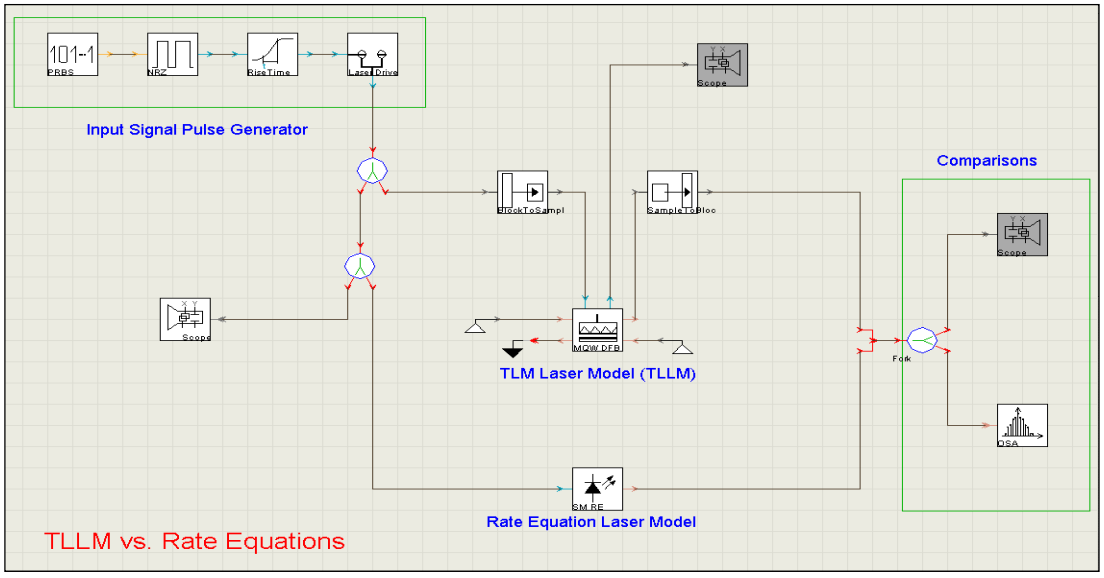

Figure 6.2 TLLM vs. Rate Equations

The system in the Figure 6.2 is driven by a pseudo random bit sequence, non-return to zero modulator, and rise time generator. The Gaussian output pulse is used to modulate laser models. The comparison of the cases is analyzed via scope signal in time domain and via spectrum analyzer in frequency domain. In the first set of the

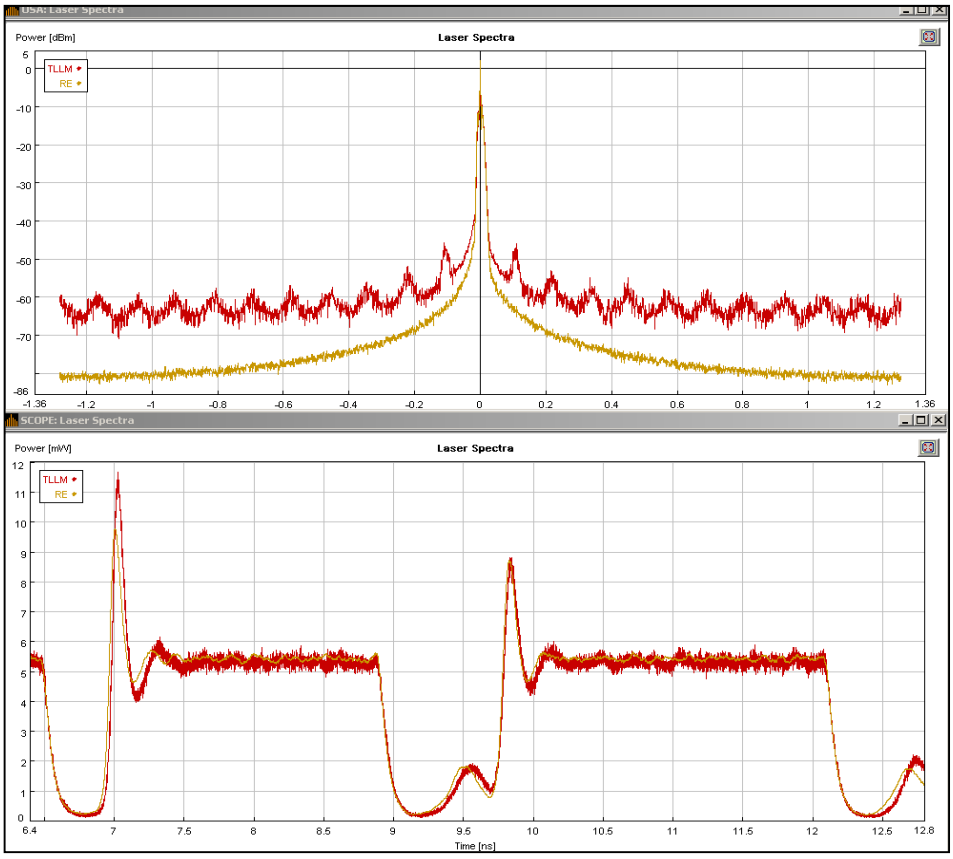

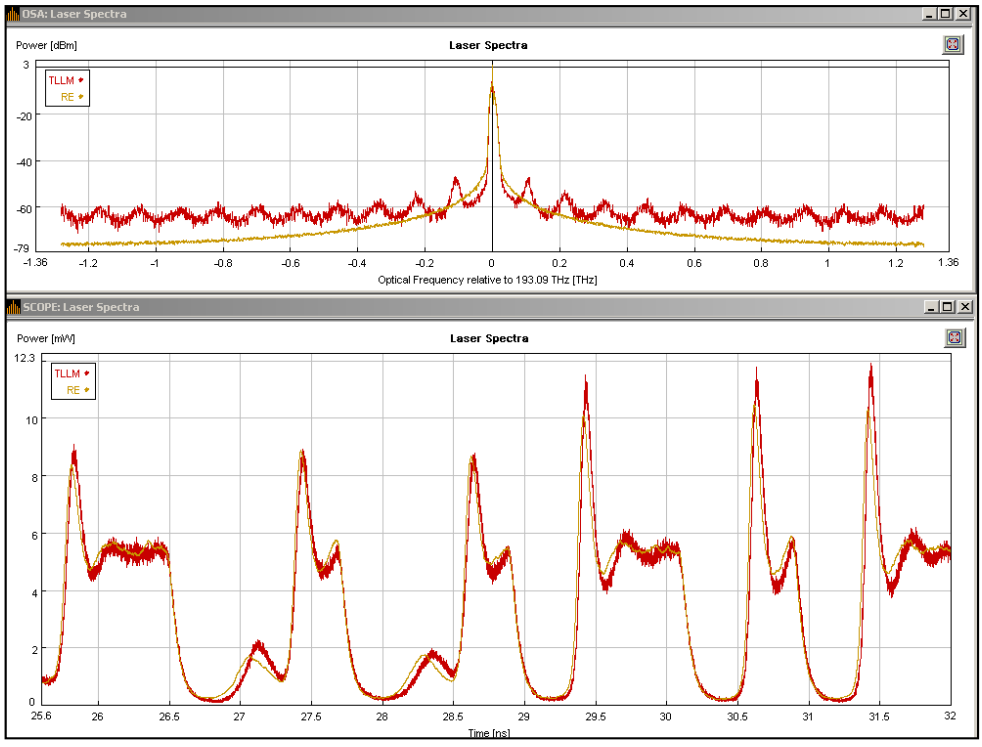

Figure 6.3 TLLM vs. Rate Equations for 2,5 Gbps and 10 Gbps Signals

simulation bit rate is 2.5 Gbps. Yellow signal shows the analytical solution of the laser rate equations and the red signal is the TLLM solution of the same system. Simulation results suits very well in the area of interest. Time domain outputs of the same system shows the consistency of the numerical TLLM solution with the analytical laser rate equations. Figure 6.3 shows the results for the 10 Gbps signal.

6.3 π-Phase Shift Analysis of SOA

All optical switches are some of the key devices in high-speed optical time division multiplexing (OTDM) systems. Mach-Zehnder interferometer (MZI) or Michelson interferometer(MI) type all optical switches with semiconductor optical amplifiers(SOA's) in their arms have been developed for stable and high speed switching. Optical logic gate operations were performed by using SOA's in an asymmetric interferometer. These devices exploit the ultra-fast nonlinearities of the SOA and the phase change, which occur when the signal passes through the SOA. A number of models and simulations are demonstrated to characterize the phase as a function of input power and bias current of SOA.

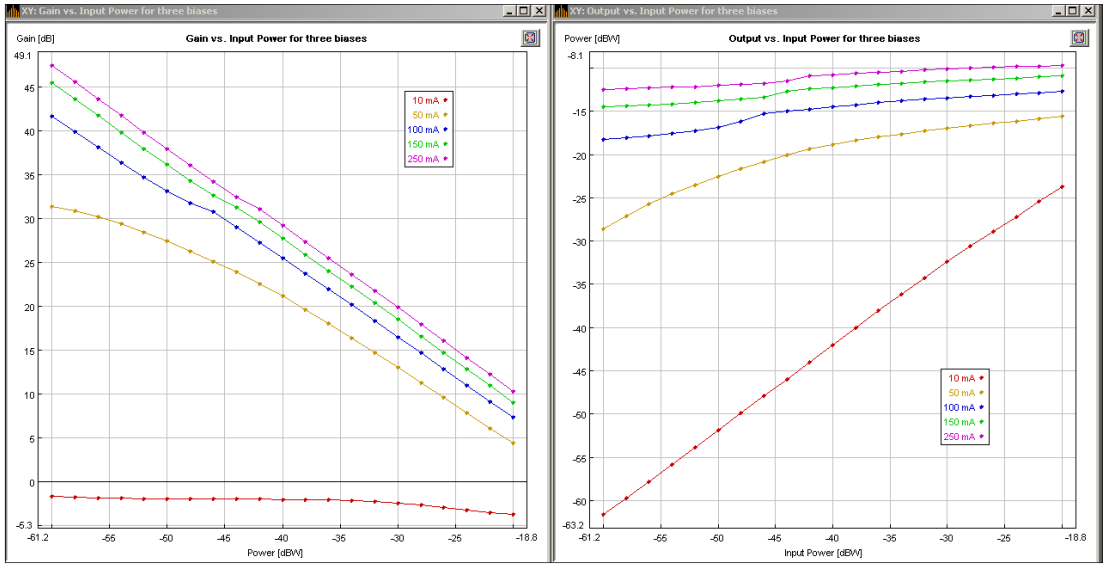

Figure 6.4 SOA Gain and Output Power vs. Input Power for three biases

Firstly, we analyze the input power versus the output power (Figure 6.4). Output power is strictly related with the bias current. The gain of SOA degrades because of the saturation of the device. The operation of SOA-based interferometric signal

processing devices relies on biasing the SOA close to its material transparency by high bias current, in a way that a π phase shift can be obtained when a signal pulse with appropriate energy level is injected. As such, the output power will increase with the control pulse energy until a π phase shift is obtained, but then greater control pulse energies will cause again an almost π phase shift leading to constant output power, since the SOA operates now at transparency(saturated) and its gain has reached unitary end-point.

Figure 6.6 shows the longitudinal-averaged carrier density for different biases. This simulation shows the main reason why we use SOA's in saturation. The switching window is the temporal transmittance of an all-optical switch. Only the part of the data signal that falls into the switching window does appear at the respective output port of the switch. Knowledge of the shape of a switching window provides information about the suitability of the device for the various signal processing applications. For sharp switching window the carrier density should change very fast.

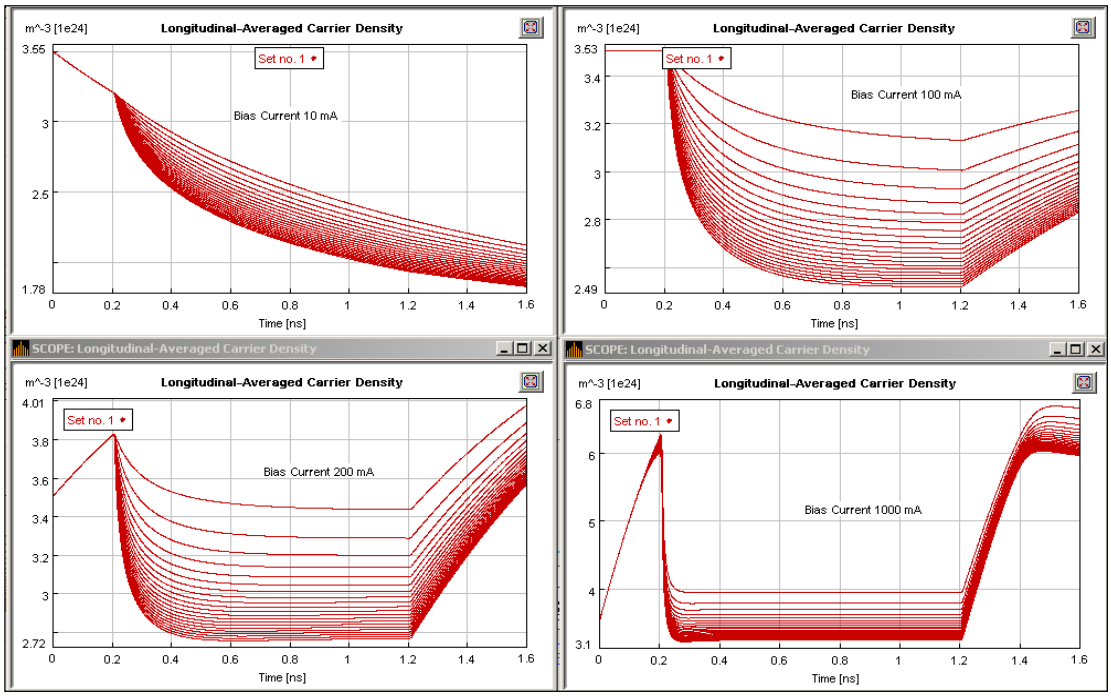

Figure 6.6 Longitudinal-Averaged Carrier Density for different biases

Another important factor is the phase of the output signal. Figure 6.7 shows the phase change for the different bias currents. For cancellation of the two signals at the interferometer output a π phase shift is required. There is a trade-off between switching window sharpness and phase difference.

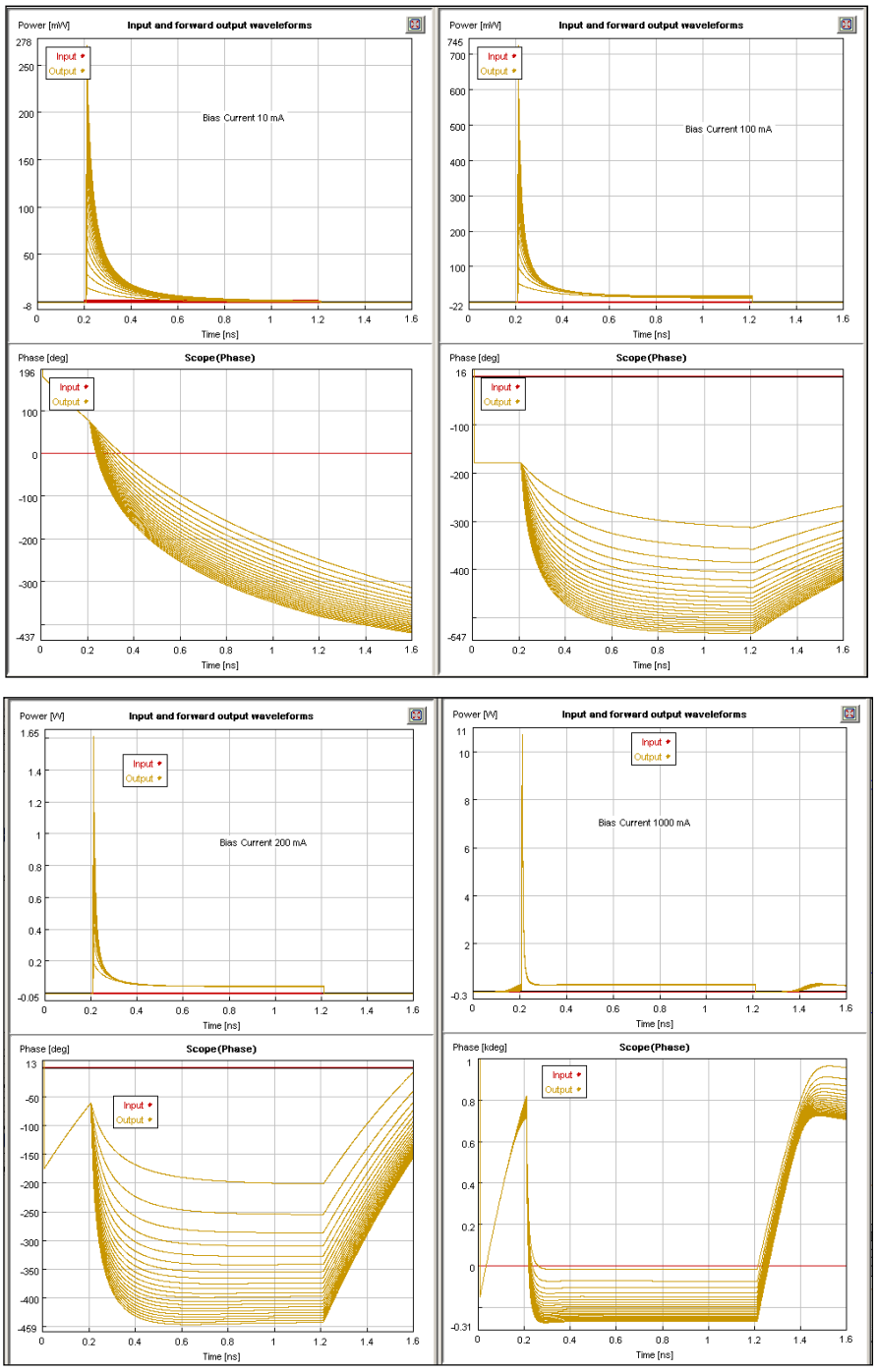

Figure 6.7 Longitudinal-Averaged Carrier Density for different biases

6.4 Sagnac-Loop Switch & Pulse Extension

Sagnac-Loop switch is another application of the SOA. Figure 6.8 shows the block diagram of the switch. There are two different probe signals entering the Sagnac-Loop via two different couplers. Two counter-propagating probe signals passes through a SOA and interfere each other at the output coupler. The nonlinear element SOA gives the pulses the required phase shift and two probe pulses switched through two different outputs of the coupler according to their phase match/mismatch. Each arm of the Sagnac-Loop has a time delay element which constructs a switching window at the output coupler. The switching window may be adjusted so that an additional pulse compression occurs.

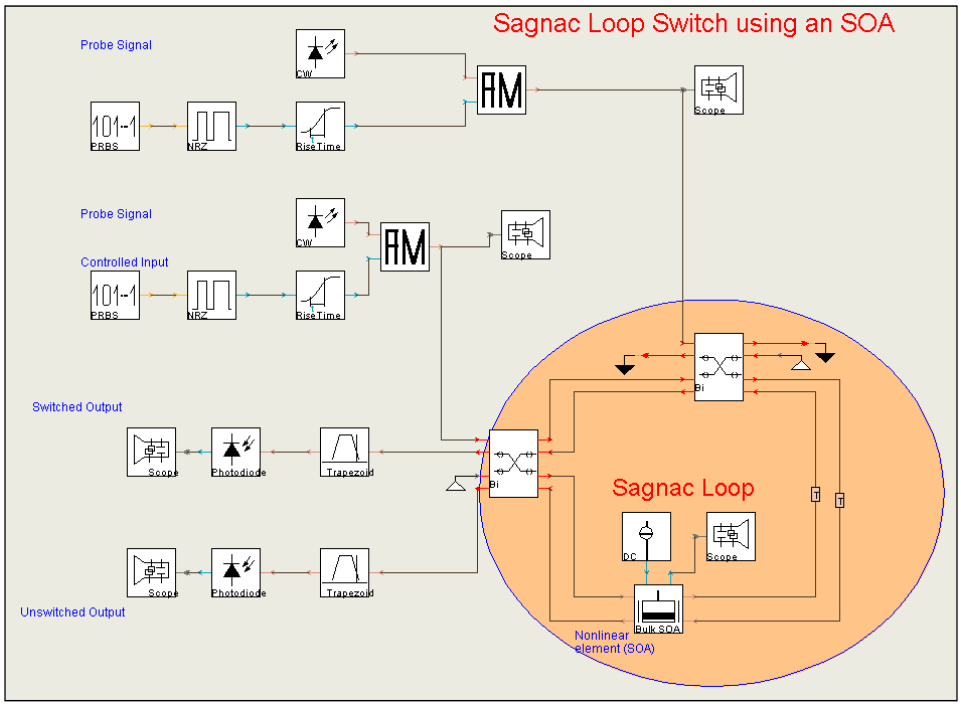

Figure 6.8 Sagnac Loop SOA Switch AND Gate

Figure 6.9 shows the simulation results of the design. In the simulation two probe signals are successfully switched between two outputs.

In our routing architecture design we need an pulse extension operation and it had been simulated with Bragg-Grating filters. Bragg-Grating filters are hard to

implement and hard to align for sensitive values. Also they require refabrication and circuit integration for different values of the pulse extension.

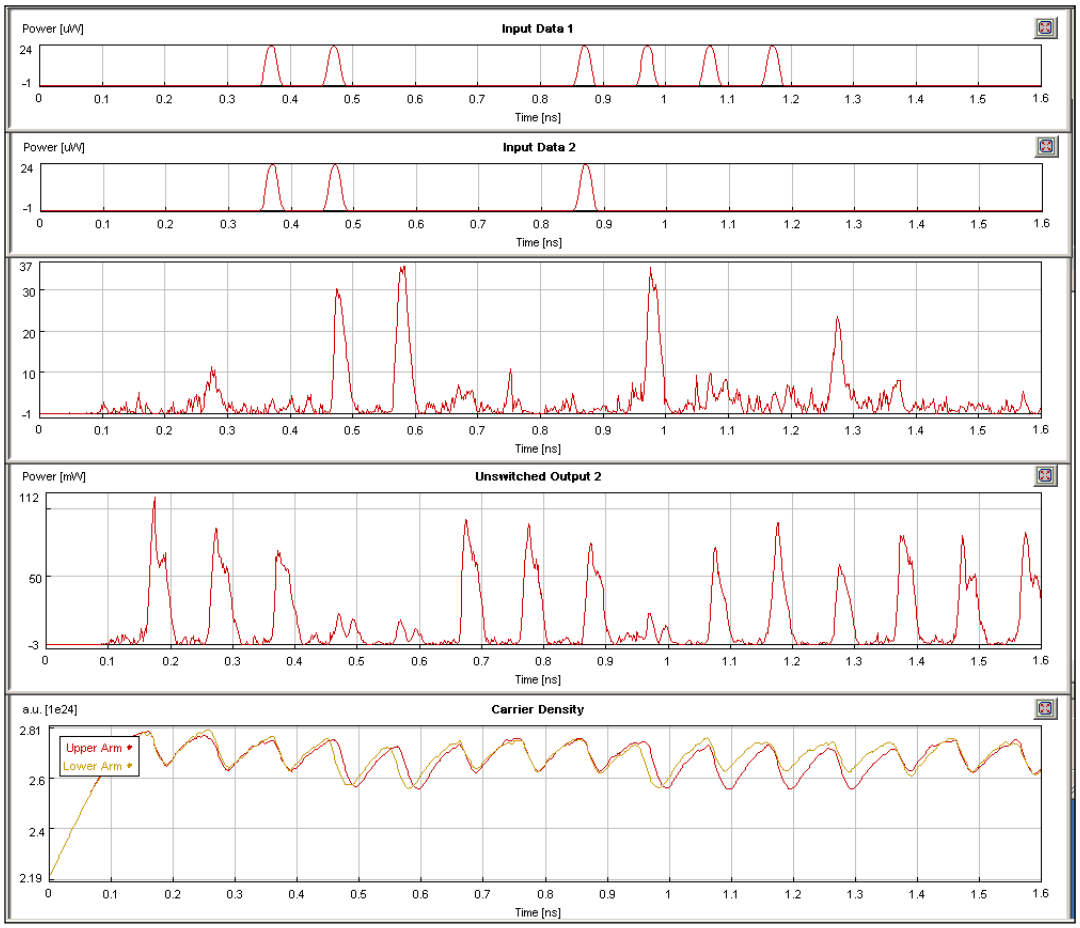

Figure 6.9 Sagnac Loop SOA Switch AND Gate Simulation Results

Sagnac-Loop switch with specific time delays may be used for alternative pulse extension operation. In Figure 6.10 Sagnac-Loop switch with specific time delays has been used for pulse extension operation. In the design, one of the two incoming pulses is set as a continuous laser input and the sum of the time delays are adjusted so that the switching window gives us the desired pulse extension duration. Figure 6.11 shows the simulation results of a pulse extension operation. The input pulse duration is successfully extended up to eight times longer in the time domain.

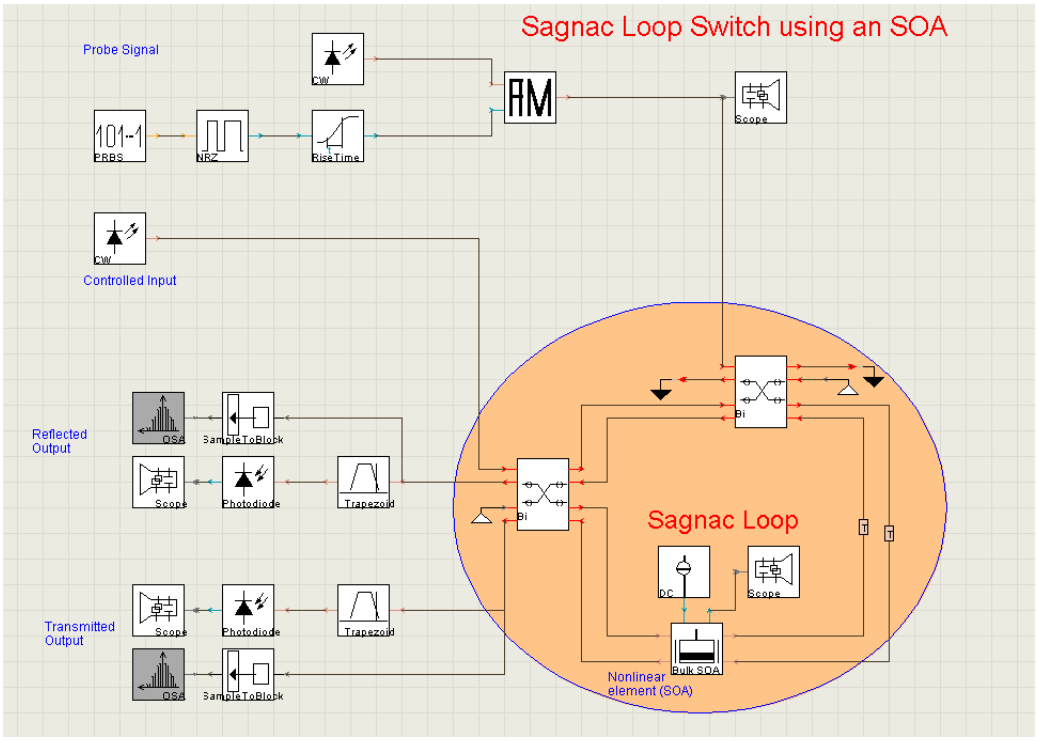

Figure 6.10 Pulse Extension using Sagnac Loop SOA Switch

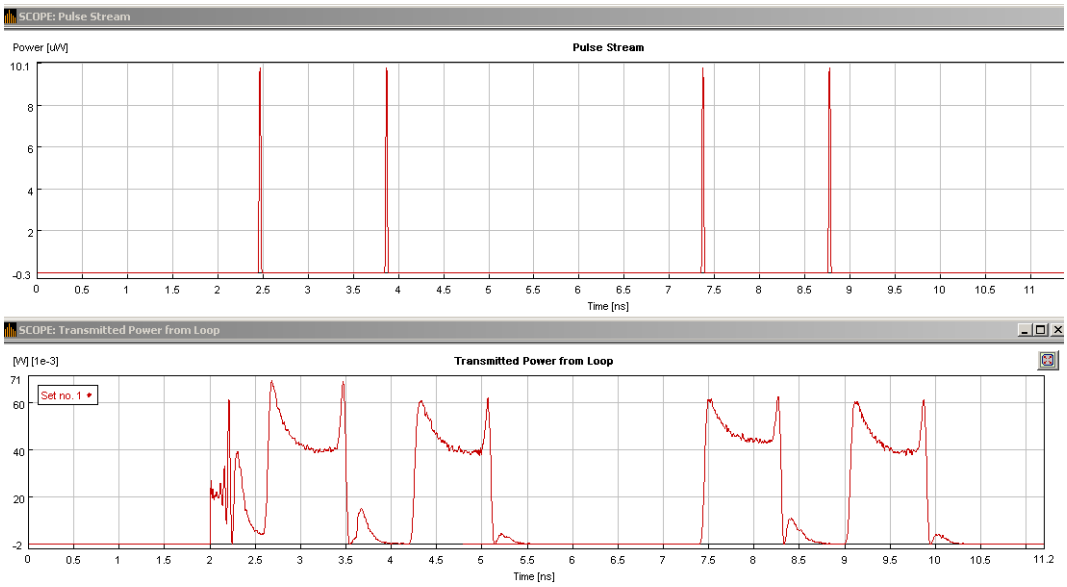

Figure 6.11 Pulse Extension Simulation Results

6.5 Noise and Jitter Analysis of the SOA Signal Processing

Xor is the most critical signal processing module in the all-optical routing architecture. Routing decision signal is generated after the XOR operation between routing table and address information of the incoming data packet.

Previous chapter included noise and jitter free analysis and simulation results of the architecture. The following simulation results are for different noise and jitter levels of the data input signal. Clock pulse stream and routing table pulse train is generated at the switching node, thus it could be assumed that there is fixed level noise for this signals.

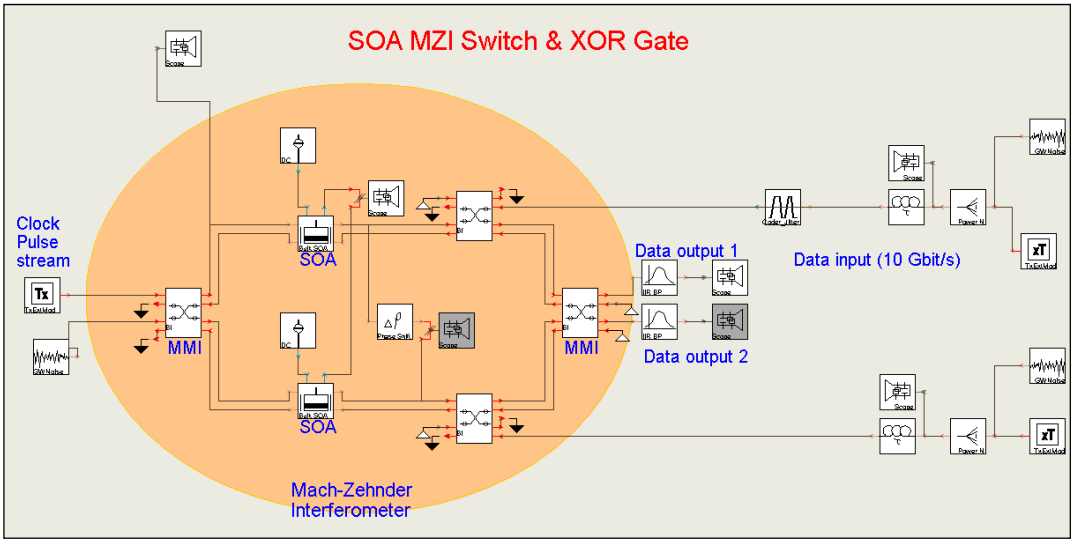

Figure 6.12 SOA-MZI Switch XOR with Noise & Jitter

6.5.1 BER Modeling

Optical systems are designed to meet requirement specifications, and one of the most common requirements is for the system to have less than a specified Bit Error Ratio (BER). Because BERs are required to be very low: between 10^{-12} and 10^{-15} commonly, the BER requirement is sometimes for the system to be “error free”, meaning less than one bit error per day at 10 Gbit/s.

The difficulty in measuring BER by counting errors is far worse for simulations, because numerical simulations take microseconds to simulate each data bit, then to simulate a system and find an error for a BER of 10^{-15} would take tens of years. However, because there are different ways to represent signals in numerical simulations, and because noise and signal can be kept as separate numerical measures (with some transmission effects being neglected), BER can be successfully

estimated in simulations with more ease than in a laboratory. The best choice of BER estimation method therefore depends on the type of system under investigation.

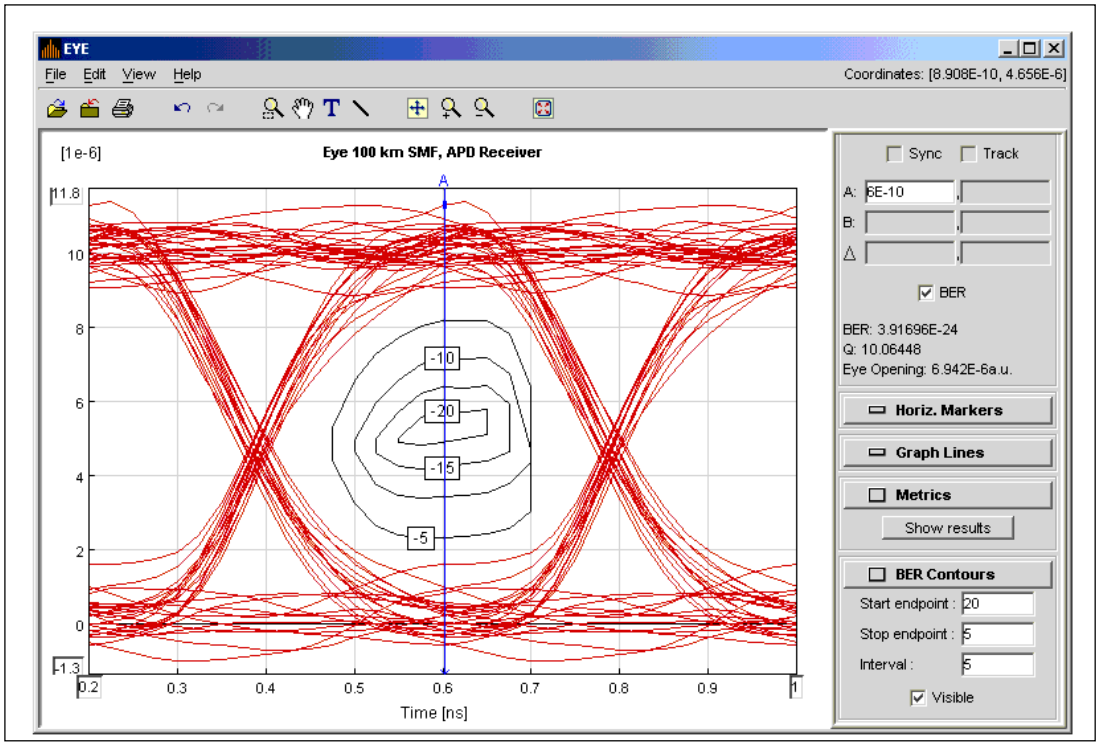

Figure 6.13 Countours of constant BER, for a 100 km SMF fiber

The input signal must have unique logical information for the calculation of BER values, plotting BER contours, finding signal metrics, and displaying eye masks. The logical information of the signal includes its bit rate and bit sequence and is usually created by the signal source. The correct BER and metrics calculations require that the received signal time shape corresponds to the transmitted bit sequence.

A mask test defines the allowable shape of the received signal waveform. This test is highly efficient since it quantifies both time and amplitude parameters in one measurement. (Derickson, 1998), (ITU-T Recommendations, 1999) By comparing an eye diagram with a predefined mask, a quality of the waveform and BER of the signal can be simply assessed (Figure 6.13).

6.5.2 Noise Modeling

White noise is a random signal (or process) with a flat power spectral density. In other words, the signal contains equal power within a fixed bandwidth at any center frequency. An infinite-bandwidth white noise signal is purely a theoretical construction. By having power at all frequencies, the total power of such a signal is infinite and therefore impossible to generate. In practice, however, a signal can be "white" with a flat spectrum over a defined frequency band.

The designed white noise module generates an optical signal where fc is the center frequency of the noise band. $\delta(\tau)$ denotes a Dirac-Delta function and P_N is the double-sided noise spectral power density. The probability density function is described by a Gaussian distribution. The module is set to produce around a center frequency of 194.05e12 Hz. The noise power density within a measurement bandwidth of 12.5 GHz is set to be 100 nW. (Figure 6.14)

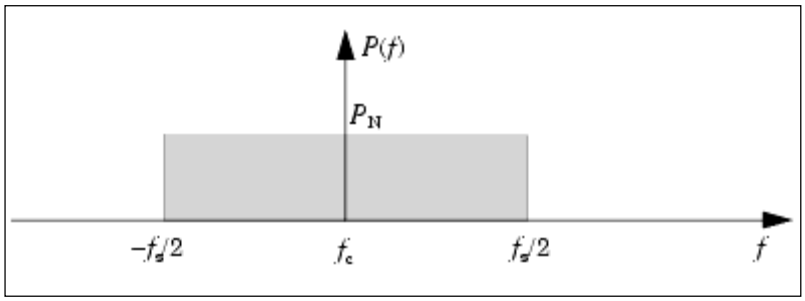

Figure 6.14 Power Spectrum of the optical White Noise source

6.5.3 Jitter Modeling

The designed jitter module generates optical signals with deterministic (sinusoidal) and/or random timing jitter. The signal jitter is modeled by means of perturbations of the clock function. These perturbations describe short-term phase variations of the significant instants of the signal (crossing points of the eye diagram) from their ideal position in time.

The timing jitter function is a subsequence of pseudorandom sequence which has a Gaussian probability distribution with zero mean and standard deviation defined by the parameter “Random Jitter Amplitude RMS”. The amplitude of the random jitter is limited by the parameter “Minimum Delay” and “Maximum Delay”. (Figure 6.15)

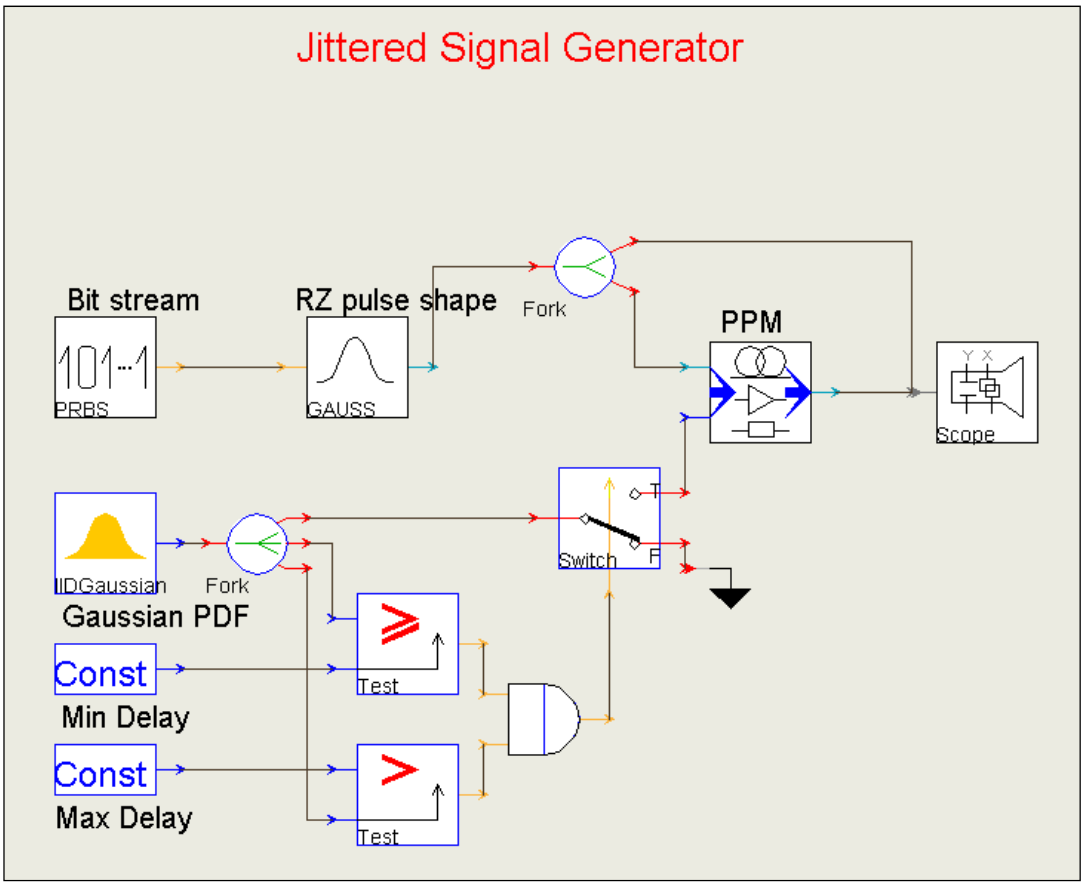

Figure 6.15 Modeling of the Random Jitter Generator

6.6 Simulation Results

The following graphs show the simulation results for the SOA XOR-Operation for different noise power spectral densities and for different timing jitters. The performance of the module is measured with BER of the output. The module is is simulated for the noise power spectral densities between 0 and 200×10^{-18} W/Hz. Figure 6.16 shows the simulation results for the jitterless and noiseless case. Switched and unswitched signals are passed through a band pass filter, so that higher and lower order frequency components is filtered.

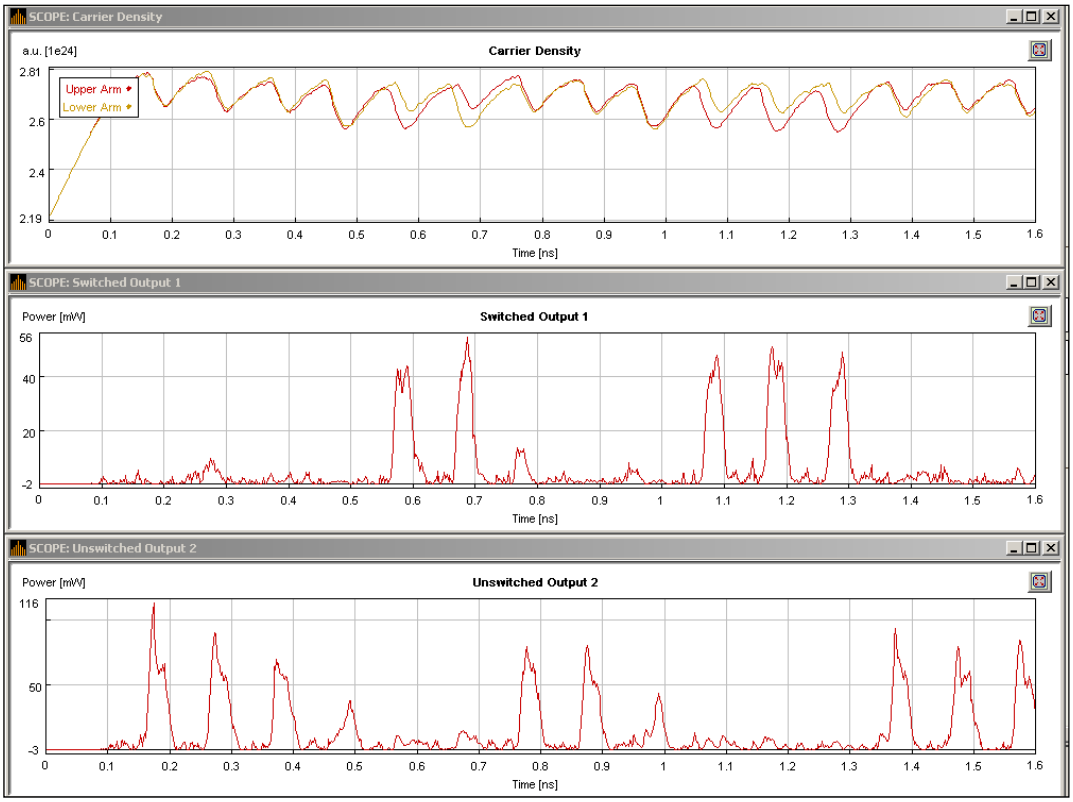

Figure 6.16 Simulation results for noiseless and jitterless case.

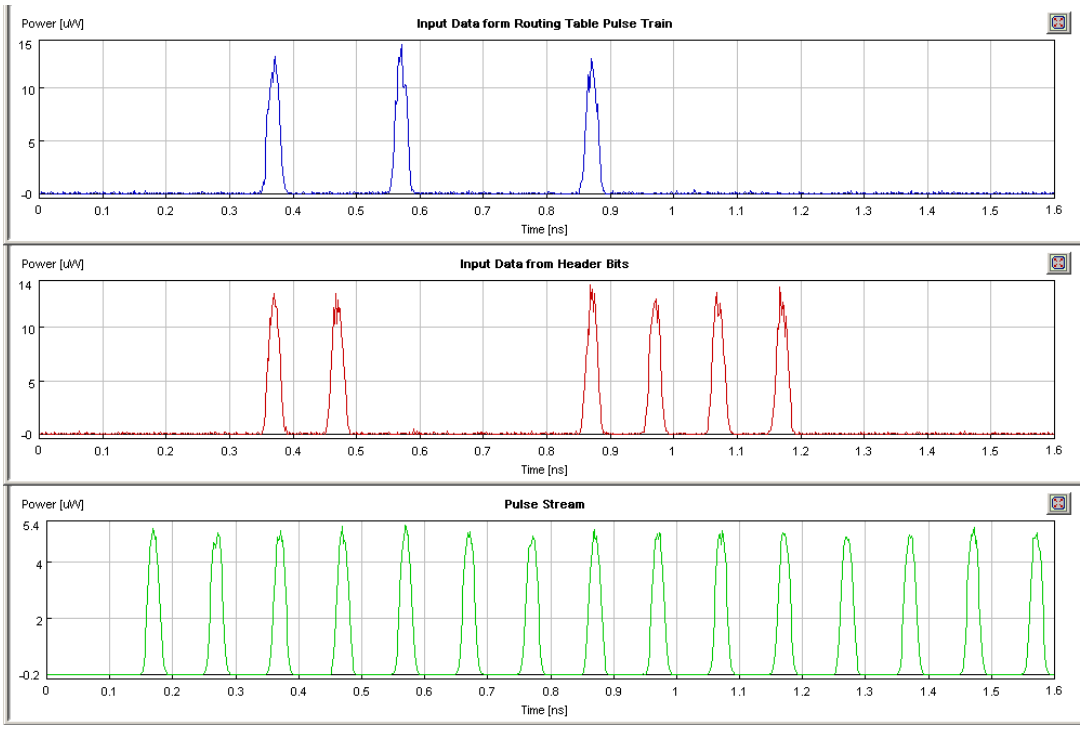

Figure 6.17 Input signals with Noise Power Spectral Density = 0

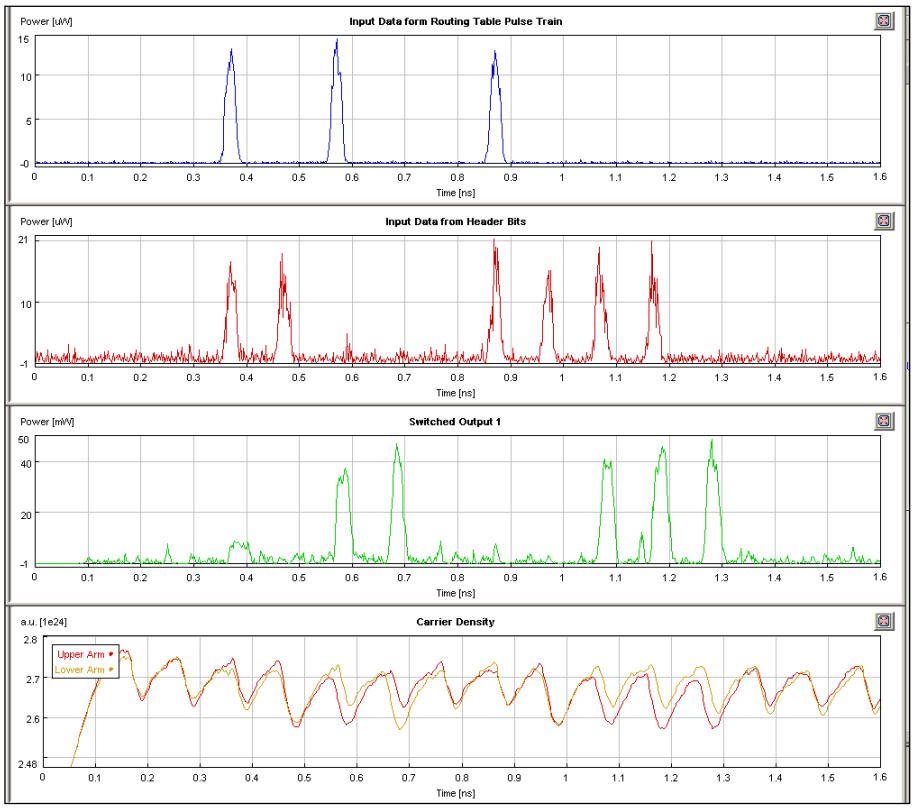

Figure 6.18 Simulation Results for Noise Power Spectral Density= $1x10^{-18}$ W/Hz

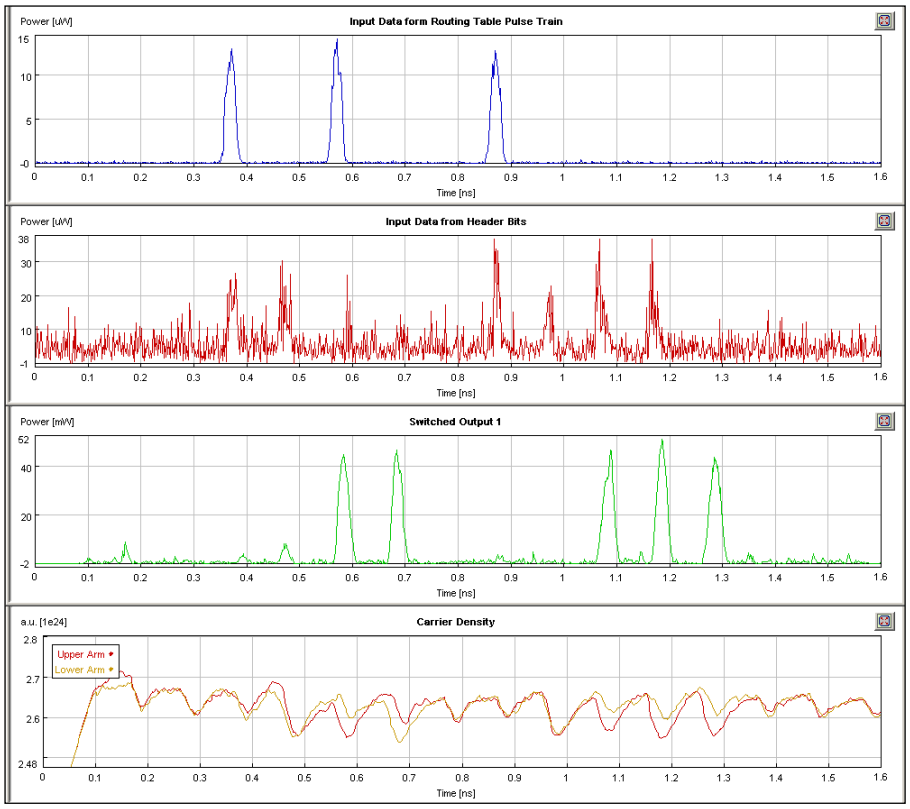

Figure 6.19 Simulation Results for Noise Power Spectral Density=$5x10^{-18}$ W/Hz

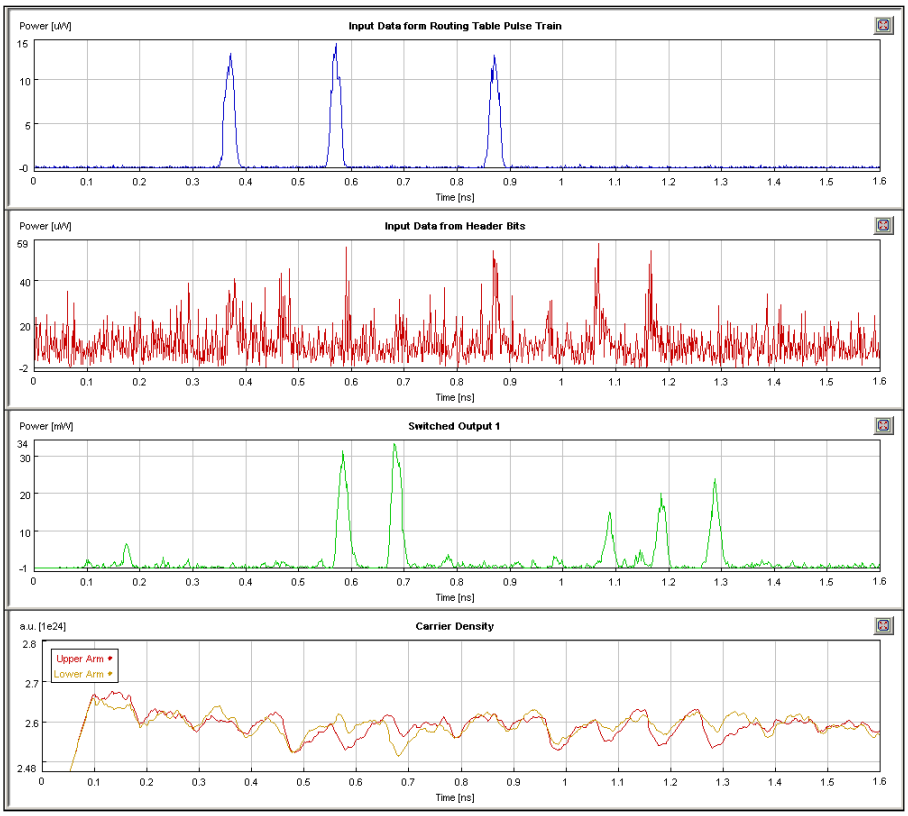

Figure 6.20 Simulation Results for Noise Power Spectral Density=20x10^{-18} W/Hz

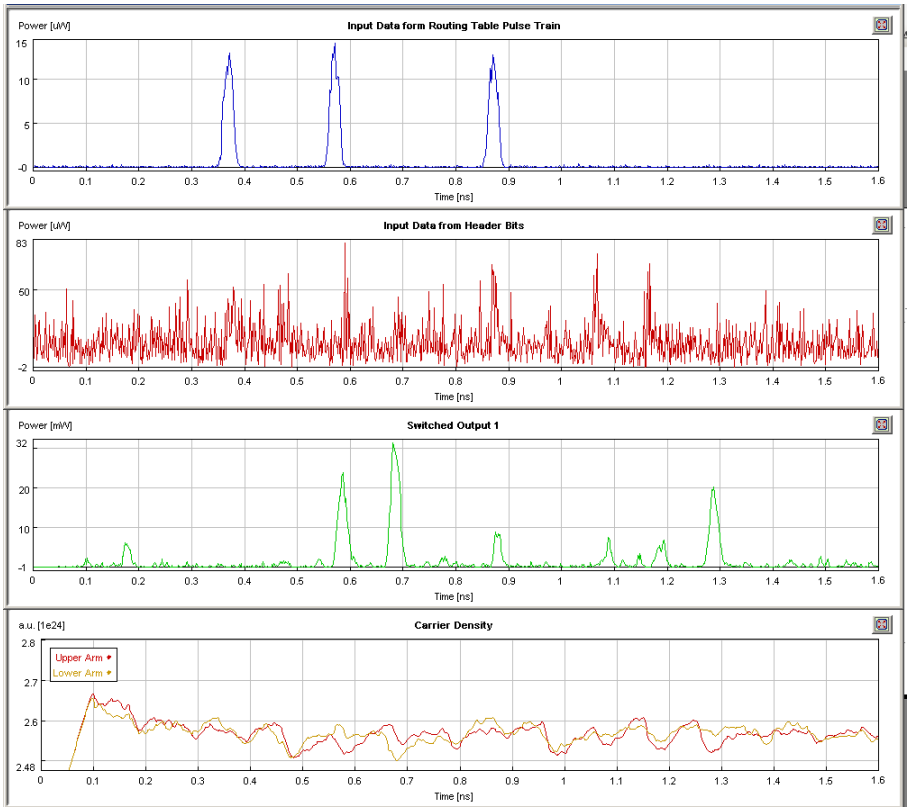

Figure 6.21 Simulation Results for Noise Power Spectral Density=100x10^{-18} W/Hz

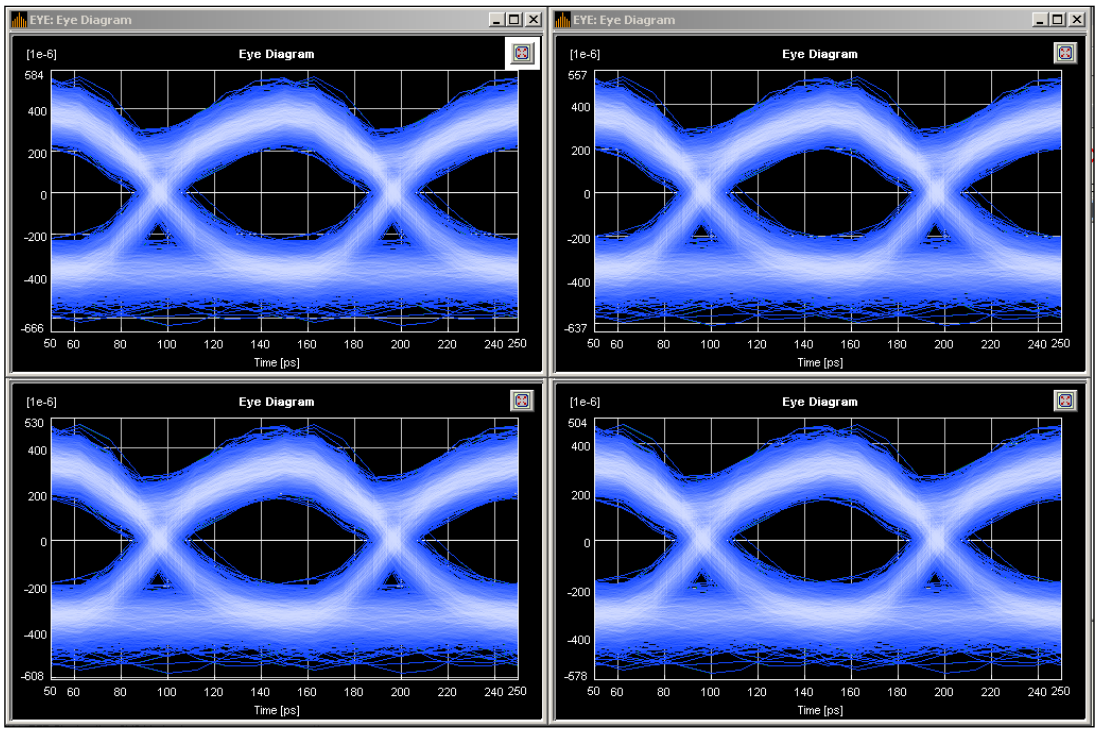

Figure 6.22 Eye diagrams for Noise Spectral Density= $1x10^{-18}$, $5x10^{-18}$, $10x10^{-18}$, $20x10^{-18}$ W/Hz

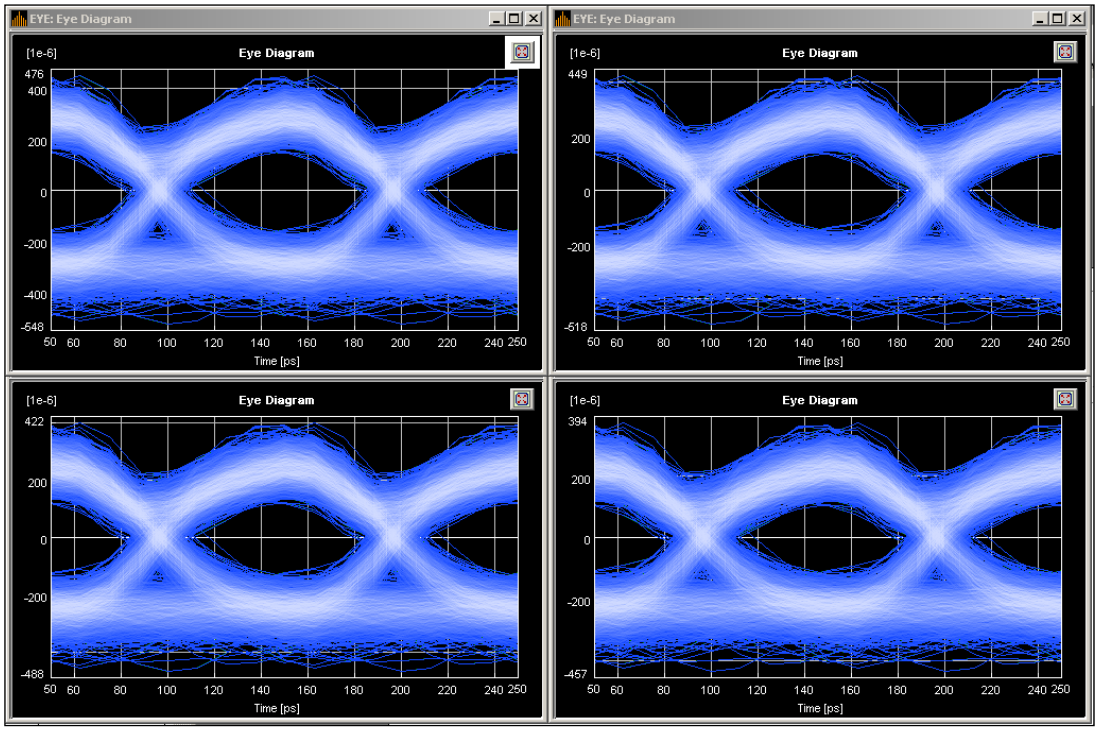

Figure 6.23 Eye diagrams for Noise Spectral Density= $50x10^{-18}$, $75x10^{-18}$, $100x10^{-18}$, $200x10^{-18}$ W/Hz

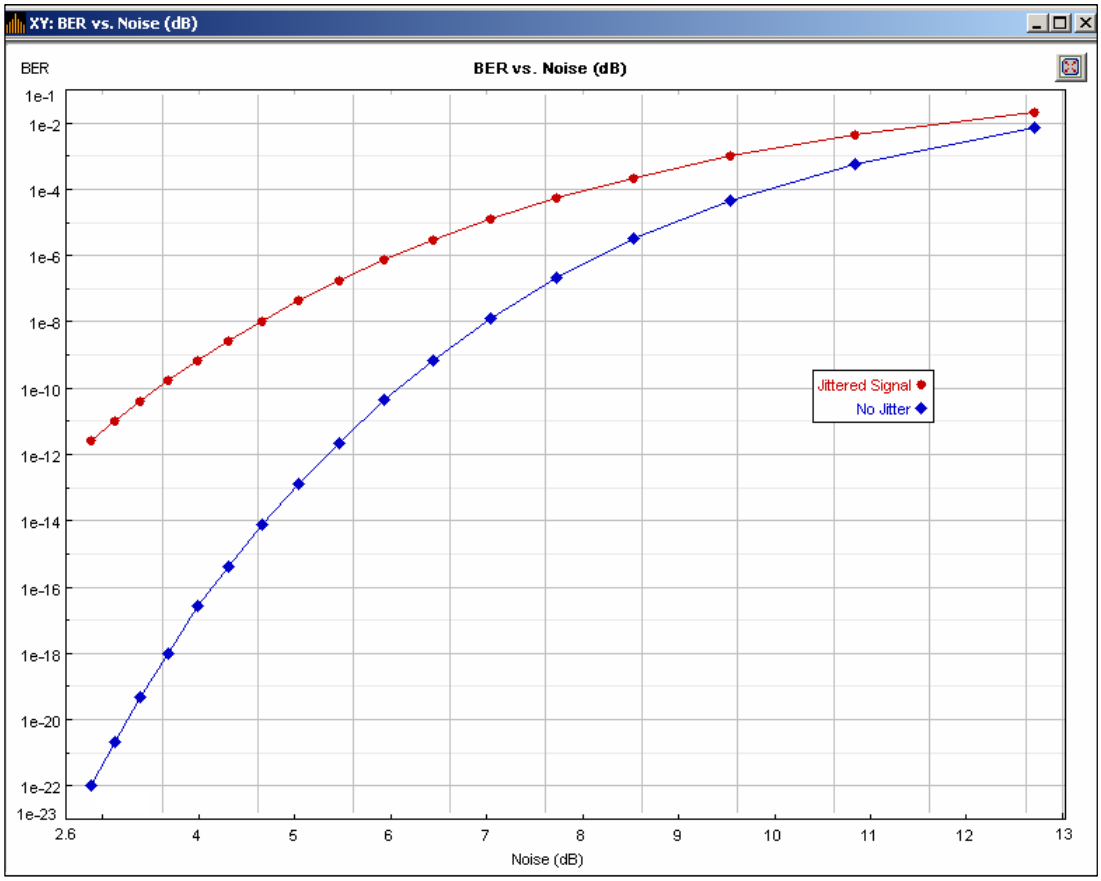

Figure 6.24 BER vs. Noise

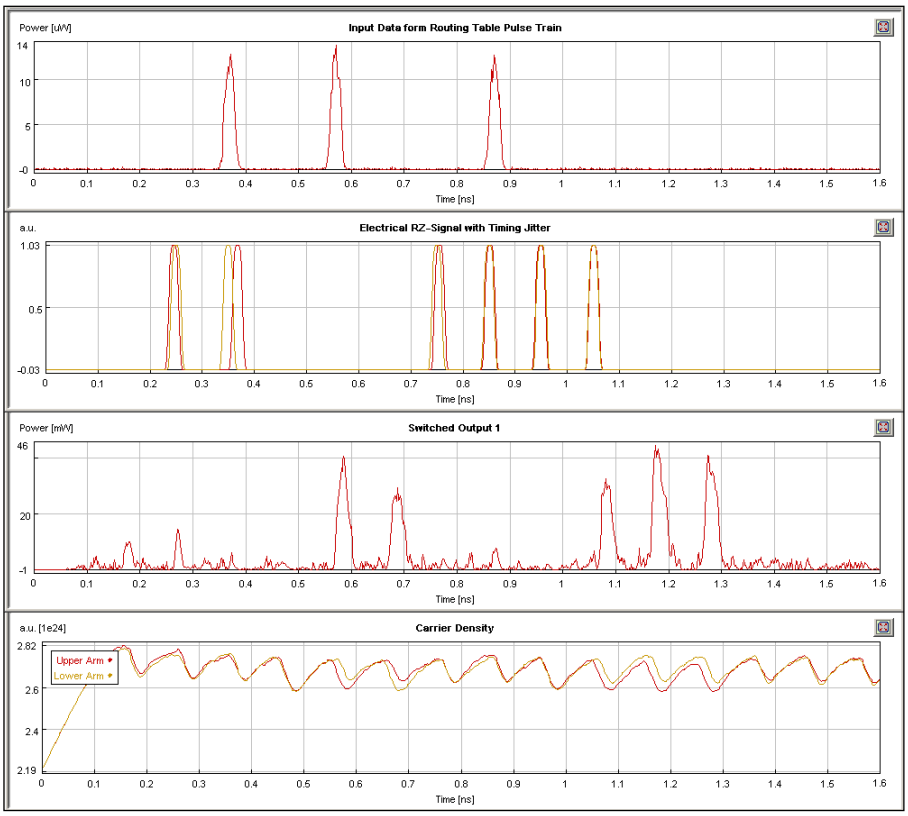

Figure 6.25 Simulation Results for RMS Timing Jitter = 0.45 ps

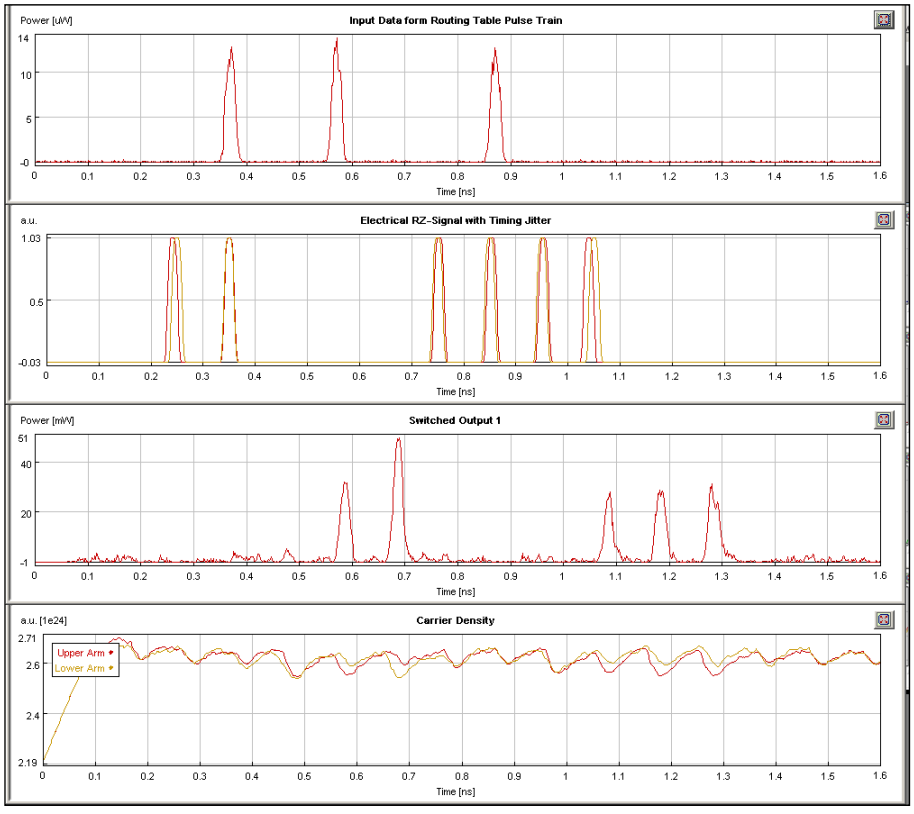

Figure 6.26 Simulation Results for RMS Timing Jitter = 0.68 ps

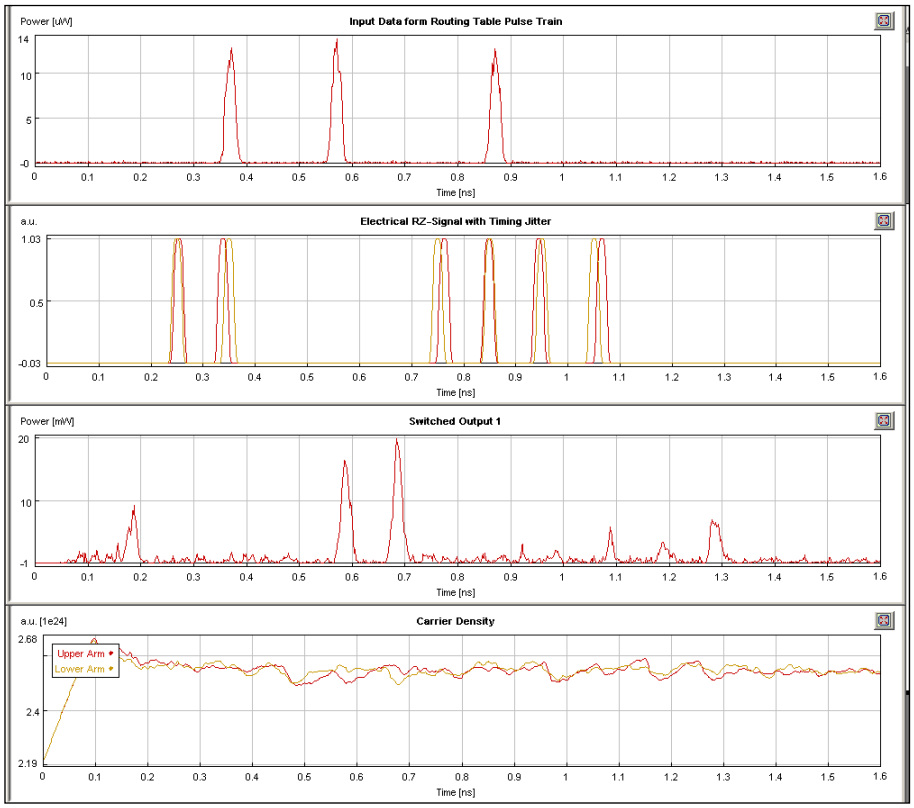

Figure 6.27 Simulation Results for RMS Timing Jitter = 0.83 ps

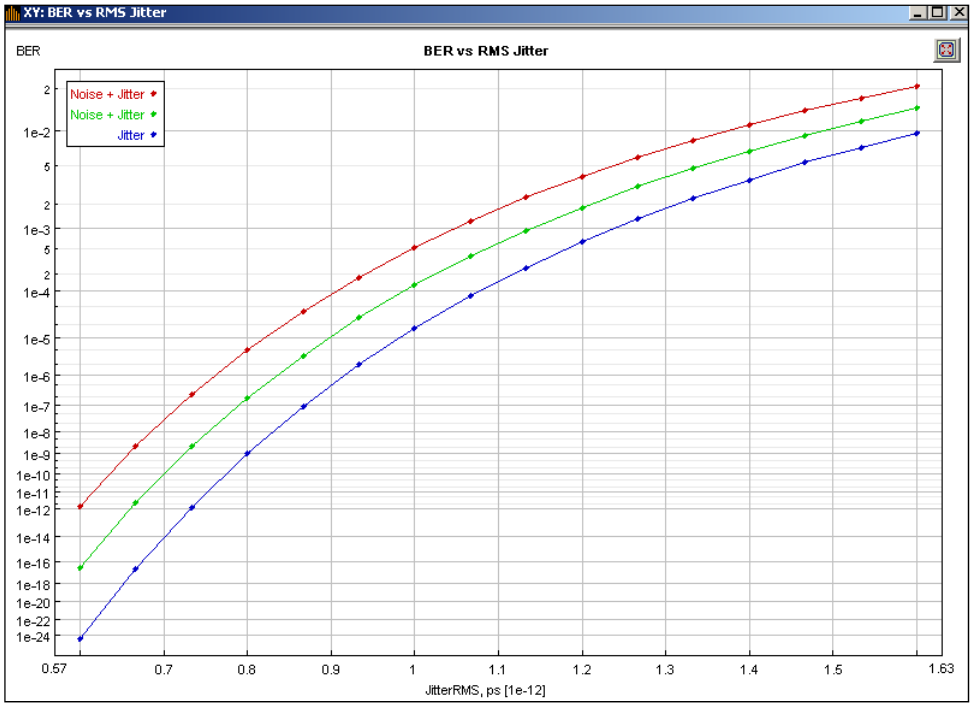

Figure 6.28 BER vs Jitter for noisy and noiseless case

The all optical signal processing of the input data signal using the proposed architecture is excellent if we assume that the propagation channel is jitterless and noiseless. However, a real channel is subject to factors such as dispersive propagation, unequal propagation in the vertical and horizontal polarization channels, and intentional or unintended signal interference, which may affect optical signals differently. Thus, a detailed BER study is essential to understand the limitations of the architecture in a realistic scenario. As stated earlier, the signal at the receiver may have errors during propagation.

The performance of the architecture in an additive white Gaussian noise (AWGN) channel is shown in Figure 6.24. The system shows excellent performance, with a probability of error of 10^{-22} at a noise power spectral density of $1x10^{-18}$ W/Hz. The differential amplitude and noise variation is not as crucial as the timing jitter because the architecture is designed to synchronous signal processing BER of 10^{-12} may be achieved at the same noise power spectral density with the rms timing jitter of 0,6ps.

The performance of the architecture in Gaussian distributed jittered channel is shown in Figure 6.28. The systems performance strongly depends on jitter level. %1 increase in jitter level may cause 1000 times decrease in BER.

CHAPTER SIX
CONCLUSIONS

It is important for network designers to reduce the number of protocol layers being used in today's networks, while preserving the functionality. The novel all-optical routing architecture proposed in this work, operates at physical layer of the OSI while providing protocol transparency. The original data packets are routed and sent to the next network node without any data conversion, it remains unchanged. The architecture is very flexible and can be implemented into different kind of networking protocols. It could be efficiently used in autonomous systems like MPLS or in IPv6 backbone routers.

The proposed architecture has been designed using realizable optical signal processing tools. Although the techniques and devices deployed in this architecture are well known for various applications of the optical communication, in this work all these techniques have been improved and exploited to integrate an all-optical routing device.

In the simulation, data packets with 10 Gbps bit rate and 3-bit header have been routed successfully into the desired path, but the architecture has the potential to route at much higher data bit rates since every component used has the characteristics that supports up to 160 Gbps. Parallel and serial approaches of the architecture are also possible. The routing table size is another critical factor for most applications. Routing with address prefixes or a parallel approach can decrease the required routing table size for the architecture.

Synchronization of the data bits is another issue that should be addressed before practical realization of the architecture. Since, in the simulation, the laser source can be excited to fire at well-defined time intervals, which are not the case of the real networks. The delay elements in the simulation are realized by a fixed-length optical cable which may also cause a time jitter problem. However, noise and loss parameters of every component, as VPI allow, are included in the simulation. Many

optical signal processing components might suffer from stability problems because of the high data rates.

Next generation networks will most probably rely on optical networking and they require faster architectures at network nodes for optimization of the performance. The proposed all-optical architecture may be an efficient alternative for backbone routers.

REFERENCES

Anonymous, (2004), *VPI Virtual Photonics User's Manual,* http://www.vpiphotonics.com/library/ActivePhotonics.pdf, 49-58.

Boyraz, O., (2003), Time Stretch Optical Header Recognition, *LEOS 2003*, 2(1), 543-544.

Brzozowski, L. (2000), Optical Signal Processing using Nonlinear Distributed Feedback Structures, *IEEE Journal of Quantum Electronics*, 36(5), 550-555.

Brzozowski, L. (2001), All-optical Analog-to-digital Converters, Hardlimiters, and Logic Gates, *Journal of Lightwave Technology*, 19(1), 114-119.

Connelly, M. J. (2002), *Semiconductor Optical Amplifiers.* Boston: Springer-Verlag.

Cotter D., (2005), Self Routing of 100 Gbit/s Packets Using 6 Bit Keyword Address Recognition, *Electronic Letters*, 31(25), 2201-2202.

Davies, J., (2003), *Understanding IPv6,* Washington: Microsoft Press.

Desmeules, R., (2003), *Implementing Cisco IPv6 Networks (IPv6),* Indianapolis: Cisco Press.

Derickson, D., (1998), *Fiber Optic Test and Measurement*, New Jersey: Prentice-Hall Inc.

Dinleyici, S. & Mocan, B., (2002), Fotonik Ağ Yapıları için Optik Sinyal İşleme Elemanları, *Proceedings of IEEE SIU 2002*, 1(1), 200-205.

Erdoğan, T., (1997), Fiber Grating Spectra*, IEEE Journal of Lightwave Technology,* 15(8), 1277-1294.

Giller, R. & Manning, R. J., (2006) Recovery Dynamics of Optically Excited Semiconductor Optical Amplifiers, *Photonic Technology Letters, IEEE*, 18(9), 1061-1063.

Hoeher, W. J. R., (1985), The Transmission-Line Matrix Method Theory and Applications, *IEEE Transactions on Microwave Theory and Tecniques*, 33(10), 882-893.

International Engineering Consortium (2006), *Optical Networks Tutorial,* http://www.iec.org.tr/whitepapers.htm.

ITU-T Recommendation, (1999), G.957, 06/99.

Johns, P. B. & Beurle, R. L., (1971), Numerical Solution of 2-Dimensional Scattering Problems Using aTransmission-Line Matrix*, Proceedings Inst. Electrical Engineering, 118(9), 1086-1091.*

Kim, J. Y., Kang, J. M., Kim T. Y. & Han, S. K., (2006), *10* Gbit/s All optical Composite Logic Gates with XOR, NOR, OR and NAND Functions Using SOA-MZI Structures, *Electronics Letters,* 42(5),

Kristian, E. S., (2000), Semiconductor Optical Amplifier-Based All-Optical Gates for High-Speed Optical Processing, *IEEE Journal On Selected Topics in Quantum Electronics,* 6(6), 1428-1431.

Liu, Y., Tangdiongga, Z. L., Huug, W., Koonen, A. M. J., Kohoe, G. D., Xuewen, S., Bennion, I., et al. (2007), Error-Free 320 Gb/s All-Optical Wavelength Conversion Using a Single Semiconductor Optical Amplifier*, Journal of Lightwave Technology,* 25(1), 103-107.

Menzel, M. (2001), *Photonics.* New York: Springer-Verlag.

Mocan, B. & Dinleyici S., (2003), MPLS Ağ Omurgaları için Tüm-optik Yönlendirici Tasarımı, *Proceedings of IEEE SIU 2003*, 1(1), 79-82.

Mocan, B. & Dinleyici S., (2006), A Novel All-Optical Routing Architecture for Optical Packet Switched Networks, *Photonic Network Communications,* 11(1), 77-86.

Odom, W. (2006), *Cisco CCNA #640-507 Certification Guide.* Indianapolis: Cisco Press.

Saleh, B. E. A. & Teich, M. C., (1991), *Fundamentals of Photonics.* Canada: Wiley Interscience.

Son C. W., Kim S. H., Young M. J., Byun Y. T., Lee, S., Woo, D. H., Kim S. H., et al, (2006), Design of All-Optical Multi-functional Logic Gate in Single Format bey Using Semiconductor Optical Amplifiers, *NUSOD 2006,* 71-72.

Spiekman, L. H., Wiesenfeld, J.M., Gnauck A. H., Garrett L. D., Van den Hoven, G. N., Van Dongen, M. J. H., et al, (2000), Transmission of 8 DWDM Channels at 20 Gb/s over 160 km of Standart Fiber Using a Cascade of Semiconductor Optical Amplifiers, *IEEE Photonics Tecnology Letters*, 12, 717-719.

Stallings, W. (2007), *Data and Computer Communications* (7th ed.). New Jersey: Prentice Hall.

Stubkjaer, K. E., (2000), Semiconductor Optical Amplifier Based All-Optical Gates for High-Speed Optical Processing, *IEEE Journal on Selected Topics in Quantum Electronics*, 6(6), 1428-1435.

Tajima, K. (2003), Ultrafast All-optical Signal Processing with Symmetric Mach-Zehnder Type All-optical Switches, *Proceedings of SPIE 4998*, 21-32.

Takahashi, R., (2001), Ultrafast All-optical Serial to Parallel Conversion for Optical Header Recognition, *Optical Communication*, 4, 506-507.

Tanenbaum, A. S. (2003), *Computer Networks* (3rd ed.). New Jersey: Prentice Hall.

Tomsu, P. & Schmutzer, C., (2002), *Next Generation Optical Networks,* New Jersey: Prentice Hall.

Walrand, J., & Varaiya, P. (2000), *High-Performance Communication Networks* (2nd ed.). San Fransisco: Morgan Kaufmann Publishers.

Yang, W., Manning R. J., Webb, R. P., Giller, R., Gunning F. & Cotter, D., (2006), High-speed All-optical Signal Processing using Semiconductor Optical Amplifiers*, ICTON 2006,* 2(4), 161-165.